energies

MDPI

Article

Modeling Merit-Order Shifts in District Heating Networks: A Life Cycle Assessment Method for High-Temperature Aquifer Thermal Energy Storage Integration

Niklas Scholliers [1,*], Max Ohagen [2], Liselotte Schebek [1], Ingo Sass [2,3] and Vanessa Zeller [1]

[1] Material Flow Management and Resource Economy, Institute IWAR, Technical University of Darmstadt, Franziska-Braun-Str. 7, 64287 Darmstadt, Germany
[2] Geothermal Science and Technology, Institute of Applied Geosciences, Technical University of Darmstadt, Schnittspahnstrasse 9, 64287 Darmstadt, Germany
[3] Section 4.3 Geoenergy, Helmholtz Centre Potsdam-GFZ German Research Centre for Geosciences, Telegrafenberg, 14473 Potsdam, Germany
* Correspondence: n.scholliers@iwar.tu-darmstadt.de

Abstract

District heating networks (DHNs) are a key technology in the transition toward sustainable heat supply, increasingly integrating renewable sources and thermal energy storage. High-temperature aquifer thermal energy storage (HT-ATES) can enhance DHN efficiency by shifting heat production over time, potentially reducing both costs and greenhouse gas emissions. However, most life cycle assessments (LCAs) remain static, rely on average data, and neglect temporal dispatch dynamics and marginal substitution among heat sources for environmental evaluation. This study introduces a dynamic life cycle inventory framework that explicitly links HT-ATES-operation scheduling in DHNs with marginal life cycle data. The framework expands system boundaries to capture time-varying changes in heat composition, combines a district heating merit-order representation (distinguishing must-run and flexible capacities) with linear programming to determine least-cost dispatch, and translates marginally displaced technologies into environmental and economic consequences. Foreground inputs are derived from an existing third-generation DHN (heat demand, generation assets, efficiencies) and publicly available energy carrier cost data and are linked to consequential background inventory datasets (ecoinvent). The framework is demonstrated for one year of operation for an HT-ATES concept with 50 GWh of injected heat. Hourly resolved results identify the marginally displaced technologies and indicate annual reductions of 5.86 kt CO_2e alongside cost savings of EUR 1.09 M. A comparison of alternative operation schedules shows strong sensitivity of both economic and environmental performance to operational strategy. Overall, the proposed framework provides a replicable and adaptable basis for consequential assessment of HT-ATES operation in DHNs and supports strategic decision-making on seasonal thermal storage deployment in low-carbon heat systems.

Keywords: aquifer thermal energy storage (ATES); life cycle assessment (LCA); marginal impacts; linear program (LP); district heating network (DHN); district heating merit order; environmental analysis; economic analysis

Check for updates

Academic Editors: Simon Muhič and Ante Čikić

Received: 28 October 2025
Revised: 25 December 2025
Accepted: 27 December 2025
Published: 31 December 2025
Corrected: 10 March 2026

Copyright: © 2025 by the authors. Licensee MDPI, Basel, Switzerland. This article is an open access article distributed under the terms and conditions of the Creative Commons Attribution (CC BY) license.

1. Introduction

Environmental and economic impacts of district heating networks (DHNs) are well studied, but most life cycle assessments (LCAs) remain static, using time-invariant and

attributional (process-average) life cycle inventory (LCI) data, rather than capturing operational dynamics and marginal substitution effects in the system [1,2]. Previous research work shows that impacts depend on generation mix and allocation choices, yet operational dispatch and heat displacement of marginal technologies are hardly considered [1]. Consequently, the system-level effects of integrating emerging technologies such as high-temperature aquifer thermal energy storage (HT-ATES) [3] on the heat supply composition, defined by the district heating merit order (DH-MO) [4] remain largely unexplored.

Aquifer thermal energy storage (ATES) is a subsurface open-loop system that stores thermal energy in underground water-bearing porous rock or sediment layers (aquifers) [5]. By enabling the seasonal storage of surplus heat for later use, ATES can improve energy efficiency and reduce environmental impacts in the heating sector [6]. ATES systems are commonly implemented in urban areas due to their small surface footprint [7], providing thermal energy for buildings and increasingly serving DHNs [8,9]. The underlying principle is the cyclic storage and recovery of thermal energy in natural aquifers [5].

ATES research spans technical simulation methods [10], policy assessment [11], and global application and historical development [5]. LCAs and techno-economic studies are widely used to evaluate environmental and economic performance [10]. Daniilidis et al. [7], for instance, assess levelized cost of heat and estimate the reduction in greenhouse gas emissions for HT-ATES by comparing it to avoided heat generation from gas boilers. Zeghici et al. [12] quantify primary energy savings and greenhouse gas emissions savings when replacing a conventional fuel-based district heating system with a system incorporating HT-ATES. Pallotta et al. [13] conduct a dynamic environmental impact assessment of a low-temperature (LT)-ATES, highlighting the temporal dependence of impacts on heat demand, system performance, and the evolving electricity mix. Agate et al. [14] evaluate the environmental and economic performance of a water-to-water heat pump coupled with an LT-ATES system, serving a small district in Rome, Italy. Todorov et al. [9] examine heat production costs and thermal aquifer impacts for an existing DHN in Finland.

Despite this growing body of work, existing ATES studies exhibit substantial methodological diversity, particularly in the definition of system boundaries in cost, greenhouse gas emissions, and LCAs [10,15]. This inconsistency limits comparability across ATES studies and constraints transferability of results to broader energy-system contexts. Moreover, LCA studies focus on LT-ATES [16–20], which is primarily applied to large individual buildings (e.g., offices) [18] or small-scale district heating systems with few alternative heat supply technologies [16,20,21]. Niche applications, such as greenhouse heating and cooling combined with in situ bioremediation, have also been addressed [17]. To our knowledge, only one comprehensive LCA research report addresses HT-ATES explicitly [22]. While LT-ATES and HT-ATES share the same basic concept, storing thermal energy in groundwater for later use, important differences affect both system design and performance.

Operation is consistently identified as the dominant contributor to impacts for both LT- and HT-ATES [16–20,22–24]. However, LT-ATES is commonly applied for both heating and cooling, whereas HT-ATES does not serve cooling purposes [25]. Because most economic benefits of ATES arise from the cooling phase, environmental and economic rentability requires particular attention when ATES serves heating only [26]. In addition, higher storage temperatures and integration into large-scale applications such as high-temperature DHNs increase system complexity [27]. In DHNs with multiple heat-supply technologies, interactions are shaped by technical and economic constraints [24]. The network effectively operates as a local marketplace [28], in which technologies compete based on marginal costs [4]. This competition determines dispatch, influences the operational schedule of HT-ATES and competing technologies, and thereby drives both environmental and economic outcomes of the technology itself and the system, critically depending on which marginal

technology is displaced by the ATES at a given time [29]. To date, the extent to which HT-ATES integration into existing DHNs alters heat supply composition and associated environmental–economic impacts has not been addressed explicitly in the literature.

A further limitation is that ATES LCA studies commonly apply an attributional approach [16–20,22], assessing the share of the global burdens assigned to the technology [30]. This, however, does not answer the decision- and change-oriented question of how burdens shift as a consequence of introducing and operating HT-ATES, which implies a consequential perspective [30,31]. Simply subtracting attributional footprints, common in parts of the LCA and techno-economic literature [7,22,32,33], yields differences in average impacts and does not represent the consequences of system change [34]. Addressing consequences requires identifying the producing activities that adjust their output and the activity-internal processes involved in that change [35]. This, in turn, motivates system expansion and a functional unit that supports assessment of net effects at the system level [31]. However, prior ATES LCAs often define the functional unit as "heat supplied by ATES" for comparison with other technologies, which tends to overlook displaced or substituted technologies within the heating system [16,17,22]. Similarly, many studies estimate avoided emissions using average emission factors [7,12,13], while the explicit system perspective, i.e., which technologies are displaced and when, remains largely absent in ATES LCA and is only partially addressed in economic assessments that focus primarily on levelized cost of heat [7,15,36].

Operational interdependencies between ATES and DHNs are therefore mostly studied from a technical performance perspective, with limited environmental and economic quantification. For example, Remmelts et al. [37] evaluate HT ATES performance in combination with a DHN under alternative operation schedules, showing that these largely influence storage capacity. Réveillère et al. [38] analyze how integrating HT-ATES affects the energy mix of a low-temperature DHN in Paris using a dynamic HT-ATES model over 30 years of operation. However, the study relies on weekly average heat loads, does not resolve demand peaks, and provides limited insight into interactions among heat providers, costs, or environmental impacts. Where displaced technologies are considered in the literature, they are often not characterized at sufficient temporal resolution to identify which technologies are displaced at which times.

In consequential assessment, identifying marginal technologies is central and is naturally supported by merit-order frameworks [35]. Opel et al. [39] estimate the annual greenhouse gas emission reductions from integrating HT-ATES at Leuphana University of Lüneburg by considering changes in existing technologies, but the analysis emphasizes technical effects rather than economic merit-order dispatch. Yet economic drivers can fundamentally alter dispatch and should therefore be represented explicitly alongside technical constraints.

Finally, system change should be evaluated using marginal effects rather than average effects [30,31,35,40]. In this context, the distinction between short- and long-term marginal effects is central to consequential LCA [30]. Short-term effects reflect changes in utilization of existing production capacity, whereas long-term effects reflect structural adaptations such as production capacity expansion [30,41]. Energy systems are often analyzed using short-term effects [31], although Eriksson et al. [42] argue that a more complete assessment is obtained when both short- and long-term options are considered. In addition, transparency regarding the system model and background data is limited in the ATES LCA literature. For example, only Moulopoulos [18] explicitly specifies the ecoinvent system model applied [43], leaving key LCI assumptions unclear in many studies.

Overall, the detailed environmental–economic implications of integrating HT-ATES into DHNs remain insufficiently explored. Existing studies often apply inconsistent system

boundaries and functional units and generally omit dispatch dynamics and marginal substitution effects, particularly in DHNs where multiple heat providers contribute to the heat supply and may be displaced simultaneously. Consequently, the literature provides limited insight into the real-world environmental and economic consequences of HT-ATES operation within interconnected heat supply systems.

To address these gaps, this study proposes a framework that explicitly links DHN operation, HT-ATES dynamics, and marginal LCI data to capture the causal environmental–economic consequences of HT-ATES integration. It thereby extends predominately LT-ATES-focused LCA research to the operational interaction of HT-ATES with existing DHNs. Accordingly, the study is limited to the operational phase and addresses the central research question: What are the environmental and economic implications of altering the heat supply composition when integrating HT-ATES into existing district heating networks?

Specifically, the work contributes the following elements:

- It adapts a consequential perspective, in contrast to predominantly attributional approaches in the existing literature, enabling decision-making and change-oriented assessment.
- It applies system expansion and a heating-system-wide functional unit to capture changes in heat supply composition across existing technologies, enabling causal net-impact assessment and improving consistent cost and emission accounting.
- It integrates a dynamic DHN-HT-ATES model to represent time-dependent technical performance relevant for LCA and economic assessment (notably schedule-dependent losses and capacity constraints).
- It adapts the DH-MO of Moser et al. [4] by distinguishing must-run and flexible capacities to identify the time resolved marginally displaced heat mix and associated costs and emission variations; the DH-MO is implemented within a merit-order dispatch model formulated as a linear program (LP).
- It quantifies environmental impacts using a hybrid approach that combines short-term operational impacts with long-term economy-wide effects, specifying the marginal technologies involved and the marginal data used [35].

The proposed framework thus captures causal operational interactions and complex marginal effects, enabling a more precise and realistic quantification of environmental and economic outcomes. It thereby links techno-economic analysis and consequential environmental assessment, providing a robust basis for evaluating the systemic impacts of thermal storage operation in DHNs.

The methodological details are presented in Section 2, which outlines key definitions, methodological adaptations, and a computational workflow in a stepwise manner. Section 3 applies and demonstrates the proposed framework through a case study of an existing DHN in Germany. The subsequent discussion in Section 4 contrasts the results with alternative operation schedules, tests robustness with a sensitivity analysis, and highlights methodological limitations. The conclusion in Section 5 summarizes results and provides an outlook for future research directions.

2. Materials and Methods

Sections 2.1 and 2.2 establish the conceptual basis of the framework by defining system boundaries and the functional unit (Section 2.1) and by formulating the DH-MO representation with must-run and flexible capacities (Section 2.2). The computational workflow is then described in Sections 2.3–2.6: technology specifications and parameter derivation are defined (Section 2.3), the dynamic DHN-HT-ATES representation is formulated (Section 2.4), and the LP dispatch model is provided to solve for the reference and HT-ATES integration scenarios to obtain hourly operation schedules (Section 2.5). The resulting

dispatch deltas, technology-specific changes in heat generation (additional/displaced) and the charging electricity demand, form the interface to the consequential LCA step, where they are linked to marginal LCI datasets to quantify environmental and economic impacts (Section 2.6). Finally, Section 2.7 provides the case study parameterization used to demonstrate Sections 2.3–2.6.

2.1. System Expansion and Functional Unit

We expand the system boundaries from a technology-specific heat output to a system-wide perspective. Whereas previous studies assess the average impacts of producing one unit of heat (e.g., $x_{HT-ATES}$, where x denotes heat output, Figure 1) [16] or consider the displacement of district heating as a single heat source [3], our approach accounts for changes in heat output across several technologies within the DHN. The assessment focuses on changes in the timing and composition of heat production and storage operation under fixed district heating infrastructure and demand conditions. Because the intervention alters the technology composition used to supply a given heat demand (rather than changing total heat delivered), the change is considered incremental [44].

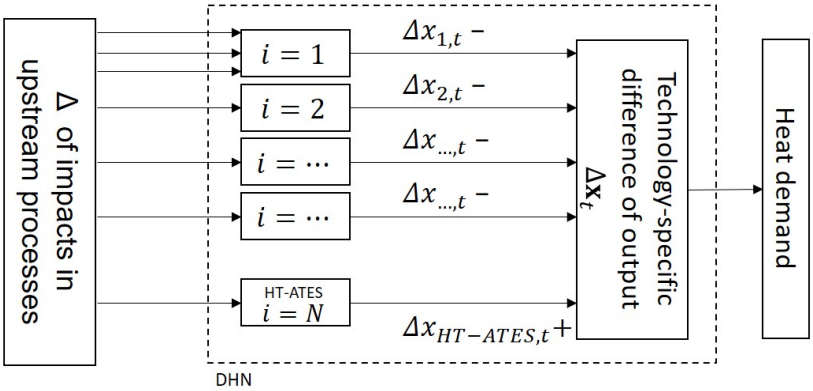


Figure 1. System expansion for assessing high-temperature aquifer thermal energy storage (HT-ATES) integration in a district heating network (DHN). The arrows denote marginal flows, and $\mathbf{\Delta x}_t$ denotes the vector of differences in the flexible output composition (Δx: flexible output difference, i: heating technology, t: time interval).

The system boundaries are defined to capture short-term operational and marginal substitution effects induced by the integration of HT-ATES within an existing DHN in the foreground system. Long-term economy-wide capacity adaptions induced by additional or lower energy carrier demands crossing the DHN's system boundaries are assessed with associated datasets in the background system (Section 2.6).

The approach reflects the assumption that the DHN operates as a constrained market in which heating technologies compete based on marginal costs, consistent with merit-order dispatch frameworks commonly applied in DHN modeling (e.g., [45–47]). Heat output composition of the existing system reacts to the decision of operating a new technology. This change, in Section 2.5 defined as the difference vector of flexible output composition at time t, ($\mathbf{\Delta x}_t$), consists of the heat supply change in each technology, in Section 2.5 defined as the flexible output difference Δx of technologies i to N at time t.

The functional unit is defined as *a technical system that covers the heat demand of the DHN at any given time* and is further specified *for over a period of one year* in the example (Section 3). It can be fulfilled with various systems, of which we assess the net difference between the reference scenario excluding HT-ATES (the system as it is) and the integration scenario. Heat demand and consumer prices are treated as equal across scenarios, owing to

the monopolistic characteristics of DHNs [4], long-term contracts, and technological lock-in effects [45,48].

Index t in Figure 1 indicates the temporal dependency on demand and marginal costs, resulting in time-varying aggregated cost and environmental impacts. The positive and negative signs denote that an increase in heat provision from the HT-ATES across scenarios necessitates an equivalent reduction in the combined output of other technologies to preserve the heat demand–supply balance.

Network heat losses are not modeled explicitly but are implicitly reflected in the storage capacity (Section 2.4). Long-term infrastructure and behavioral changes within the DHN, such as pipeline refurbishment or expansion, changes in the supply temperature regime, and user-side heat demand response, are outside the scope of this study and therefore not considered.

2.2. Adaptation of the District Heating Merit Order

The DH-MO model, conceptualized by Moser et al. [4], serves as a prioritization framework to identify a short-term marginal technology in a DHN, the technology adjusting its output to meet short-term fluctuations in heat demand. The DH-MO ranks technologies by their ascending marginal cost (EUR/MWh) on the vertical axis and plots them against current heat output (MWh) per time interval on the horizontal axis. Each technology is represented by a bar whose width corresponds to its available thermal output. The marginal technology is determined by the intersection of the aggregate bars with the network's heat demand.

We adapt the DH-MO to focus on time dependent demand, covered by flexible technologies [49], excluding must-run capacity that operates irrespective of demand [50,51] (Figure 2). Integrating an additional technology into the system eventually alters the flexible part of the merit order and the heat supply composition across technologies. The DH-MO is used to identify the technologies changing supply and their respective flexible amount. The x-axis unit is MWh, representing the amount of heat one technology can provide during one assessed time interval. The y-axis unit is EUR/MWh, representing the marginal cost per unit of heat provision during the same time interval. The bar areas represent the variable cost per technology to cover flexible heat demand, not covered by must-run capacities. We provide the following definitions:

Aggregate available capacity (MWh) is the maximum amount of heat all technologies within the DHN can provide. It differs from installed capacity in that not all installed capacity is available at any time, particularly the installed capacity of renewables or storage systems. Aggregate available capacity is the sum of available capacities $x_{\mathrm{av},i,t}$ (MWh) across technologies at time t.

Aggregate must-run capacity x_{run} (MWh) is the portion of aggregate available capacity that is technically or contractually non-dispatchable. It is the sum of must-run capacities $x_{\mathrm{run},i}$ (MWh) across technologies and is assumed constant in this model.

Aggregate flexible capacity $x_{\mathrm{flex},t}$ (MWh) is the portion of aggregate available capacity that can be modulated or turned off at time t. It is the sum of flexible capacities $x_{\mathrm{flex},i,t}$ (MWh) across technologies at time t and therefore the difference between available capacity and must-run capacity.

Aggregate output (MWh) is the heat output of all individual heating technologies at time t to cover the heat demand $x_{\mathrm{d},t}$ (MWh). The aggregate output equals heat demand at most times but can be larger in low-demand times due to must-run constraints.

Aggregate must-run output (MWh) is the heat output of aggregate must-run capacity and equal in size. It is the sum of must-run output across technologies. Aggregate

and individual must-run output of technologies are considered to be of equal size in both scenarios.

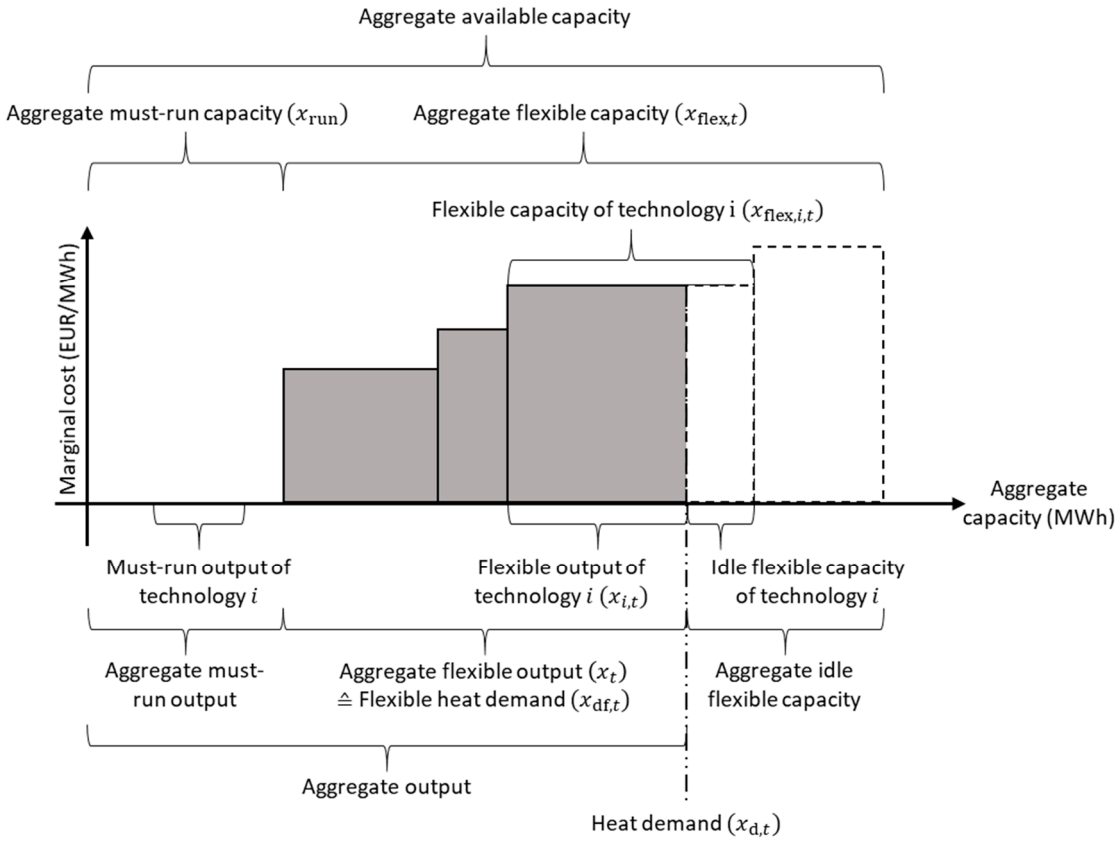


Figure 2. District heating merit order (DH-MO), adapted from Moser et al. [4], applied to aggregate flexible capacity $(x_{\mathrm{flex},t})$.

Aggregate flexible output x_t (MWh) is the output that flexible capacities provide at time t. It is the sum of flexible outputs $x_{i,t}$ (MWh) across technologies and it covers the flexible heat demand $x_{\mathrm{df},t}$ (MWh), which is the heat demand subtracted by must-run output. Flexible output is defined as non-negative, not accounting for flexible heat uptake of technologies.

Aggregate idle flexible capacity (MWh) is the unused portion of the aggregate flexible capacity at time t. It is the sum of idle flexible capacities across technologies.

The adapted method determines the marginal flexible technologies affected and their output alteration due to the operation of the HT-ATES. The following limitations apply:

- Heat demand is assumed not to change when introducing the HT-ATES; network inefficiencies (e.g., pipeline losses) are included in the available capacity of the HT-ATES.
- Marginal effects equal variable effects, assuming linear output relationships across a technology's flexible capacity.
- Excess heat output may occur if demand is lower than must-run capacities. In such cases, surplus heat generation is assumed to be technically manageable (e.g., via dissipation).
- Must-run capacities do not change due to the HT-ATES integration.

2.3. Specifications of District Heating Technologies

As the first step in the computational workflow, the district heating technologies that constitute the dispatch option space are characterized in terms of available capacity, must-run and flexible capacity shares, efficiencies, and marginal flows, together with associated

marginal costs. The parameters are later passed into the LP model (Section 2.5) as technical and economic constraints.

Technologies are indexed by $i \in \{1, 2, \ldots, N\}$, where N is the total number of technologies.

Available capacity, denoted as $x_{\mathrm{av},i,t}$, represents the maximum heat the individual technologies can deliver over a defined duration Δt (e.g., 1 h). It is calculated as:

$$x_{\mathrm{av},i,t} = P_{i,t} \cdot \Delta t \tag{1}$$

where

- $x_{\mathrm{av},i.t}$ (MWh) is the available capacity of technology i at time t,
- $P_{i,t}$ (MW) is the available heating power of technology i over duration of time interval Δt,
- Δt (h) is the duration of the time interval considered.

Technologies of the same kind are aggregated into a single entry and their available capacities summed.

Must-run capacity $x_{\mathrm{run},i}$ (MWh) represents the minimum heat generation required due to technical, operational, or regulatory constraints of technology i. The aggregate output of must-run capacity $x_{\mathrm{run}} = \sum_{i=1}^{N} x_{\mathrm{run},i}$ may exceed heat demand during low-demand periods.

Flexible capacity $x_{\mathrm{flex},i,t}$ (MWh) is the flexible capacity of technology i at time t, representing the adjustable portion of a technology's capacity, defined as:

$$x_{\mathrm{flex},i,t} = x_{\mathrm{av},i,t} - x_{\mathrm{run},i} \tag{2}$$

Marginal flows are the inputs and outputs of a heat generation process that change with an increase or decrease in heat provision. The use of marginal data in LCA is often imprecise [35], as many studies include infrastructure or other long-term capital goods that do not vary under short-term operational adjustments. For DHN-technologies, only flows that change with flexible output are considered, in line with the definition of marginal data by Heijungs [35]. The magnitude of these changes depends on technology-specific parameters such as fuel type, efficiencies, and stoichiometric ratios, which can be derived from expert consultation, literature, and life cycle inventories.

The mechanism is illustrated using a river-source heat pump (RSHP) in Mannheim, Germany, as the marginal technology. The system provides 20 MW of thermal output with 7 MW of electrical input, corresponding to a coefficient of performance (COP) of 2.9 [52]. Considering seasonal effects, a seasonal coefficient of performance (SCOP) of 2.6 is assumed for the heating period. If an additional district heating demand of $\Delta Q_{\mathrm{DH}} = 1$ MWh is covered by the RSHP operating at partial load, the corresponding electricity input is given by

$$\Delta Electricity = \frac{\Delta Q_{\mathrm{DH}}}{SCOP} = \frac{1\ \mathrm{MWh}}{2.6} \approx 0.38\ \mathrm{MWh}. \tag{3}$$

From energy conservation, the marginal heat extracted from the river is

$$\Delta Q_{\mathrm{river}} = \Delta Q_{\mathrm{DH}} - \Delta Electricity = 1\ \mathrm{MWh} - 0.38\ \mathrm{MWh} = 0.62\ \mathrm{MWh}. \tag{4}$$

Thus, per 1 MWh of marginal heat supplied, the flows comprise 0.38 MWh of electricity demand and 0.62 MWh of river heat extraction (Figure 3). These flow changes are used to calculate marginal life cycle inventories and environmental impacts (Section 2.6).

Marginal costs are obtained by assigning monetary values to the flows. Additional costs (e.g., taxes, network tariffs) are included if they vary accordingly. Hence, marginal costs represent the variable costs of flexible heating capacities per unit of output (e.g.,

1 MWh), assuming linearity across the power spectrum. These costs form the marginal cost vector:

$$\mathbf{c}_{\text{var},t} = \left[c_{i=1,t}, c_{i=2,t}, \ldots, c_{i=N,t}\right]^{\top} \quad (5)$$

where $c_{i,t}$ is the marginal cost of technology i, fluctuating at each time t.

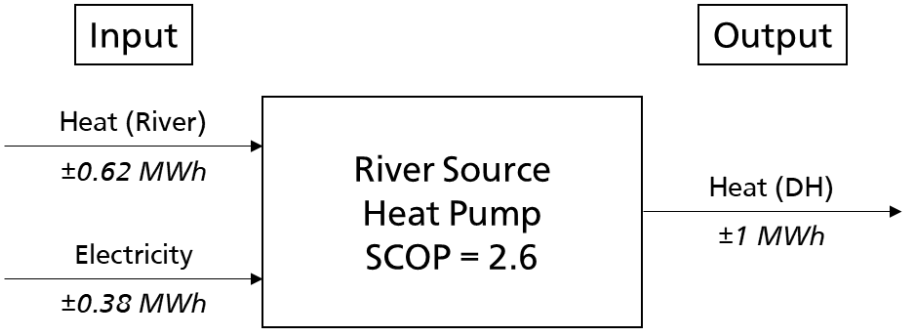


Figure 3. Marginal flows resulting from a change in heat output (example: river source heat pump).

The technologies arranged in ascending order of marginal costs form the merit order of flexible capacities. Purely must-run technologies without flexibility are denoted by "0" and are excluded in further consideration due to equal output in both scenarios.

2.4. Dynamic DHN-HT-ATES Model

The dynamic DHN-HT-ATES model provides the HT-ATES parameterization based on DHN heat demand and network temperatures. It derives annual injection and extraction capacities and annual storage losses, converts them into capacity constraints and average hourly loss parameters, and passes these to the LP model (Section 2.5). To simulate the thermal behavior and operational constraints of the HT-ATES integration, the model is developed in Modelica [53] and simulated using the Dymola 2024x [54] system modeling software. The description below provides the general application of the model, while numeric parameters of the case study are provided in Section 2.7.

2.4.1. System Topology and Components

The DHN is modeled as a simplified source-sink system designed to replicate the thermodynamic conditions of the real-world network without simulating the full hydraulic complexity of the distribution grid. The system consists of the following key components adapted from the open-source Buildings [55] and DisHeatLib [56] libraries:

- Producer: Represented as an ideal heater with unlimited capacity, coupled with a circulation pump that governs mass flow. This component imposes the network's supply temperature based on historical measurement data.
- Consumer: Modeled as an ideal cooler with unlimited cooling capacity. This component determines the heat load by cooling the working fluid down to the network's historical return temperature.
- HT-ATES Integration: The HT-ATES and its associated heat pump and heat exchangers are hydraulically connected between the producer and consumer. This configuration allows the system to extract heat from the supply line during charging and inject heat back into the supply line during discharging.

2.4.2. Hydraulics and Network Assumptions

A key simplification in this study is the exclusion of explicit pipeline distribution modeling (nodes, pipe lengths, and friction losses). This approach is justified by the use of central plant measurement data provided confidentially by a DHN operator. Because the

input temperature profiles (T_{supply} and T_{return}) were measured at the central generation plant, they implicitly account for the aggregate heat losses and hydraulic delays of the existing network. Consequently, modeling the physical pipes was unnecessary for determining the thermodynamic boundary conditions at the point of HT-ATES integration.

2.4.3. HT-ATES and Heat Pump Specification

The HT-ATES is modeled using the low-order formulation proposed by Maccarini et al. [57], which approximates the subsurface thermal response while maintaining computational efficiency. Key hydrogeological and thermal parameters used in this simulation include:

- Well Configuration: Two-well system (one warm and one cold well).
- Aquifer Properties: Aquifer thickness, porosity, hydraulic conductivity, volumetric heat capacity, and thermal conductivity. Quantitative data are commonly derived from the literature for matching geological conditions (i.e., [58]) or field studies such as exploratory drilling.
- Heat Pump: To lift the temperature from the aquifer to the required network supply levels, a heat pump is modeled using a simplified Carnot efficiency approach with a constant efficiency factor of 0.5 [59].

2.4.4. Control Logic and Dispatch

HT-ATES operation is governed by excess heat in the DHN during charging and by temperature- or cost-related constraints during discharging. Network and storage temperature constraints are first used to determine the maximum technically available discharge capacity without economic constraints. These constraints are then added in the LP formulation to implement merit-order operation (Section 2.5).

- Heat demand: Heat-demand data can be obtained in different ways. For retrospective assessments (i.e., "what if an HT-ATES had been integrated?"), historical demand data are suitable. Prospective assessments (i.e., "what if integration occurs in the future?") require scenario-based modeling. An hourly resolution is recommended, used in this study, to capture DHN operational constraints and flexibility requirements.
- Charging: Charging is enabled during the storage season (1 May to 30 September). The control logic starts the injection pump when aggregate must-run generation exceeds network demand by at least 17 MW and the charging mass flow is capped at 200 m^3/h. This ensures that costs and environmental impacts occurring due to charging are limited to the electricity consumption of the submersible injection pumps and not induced by additional heat generation. Charging operation is not affected by the merit-order-based discharging strategy.
- Discharging: Discharging is triggered after the charging season and when the HT-ATES temperature exceeds the median DHN return temperature. In the run that determines the maximum technically available discharge capacity, discharging depends only on the thermal states of the storage and the network. Economic constraints applied in the LP model then shift storage dispatch through merit-order considerations (Section 2.5).

2.4.5. Seasonal Coefficient of Performance

The SCOP of the HT-ATES heat pump is defined as the ratio of the total useful heat delivered by the heat pump to its electrical energy consumption over the discharge period using hourly simulation results:

$$SCOP = \frac{\sum_{t=1}^{T} Q_{HP,out,t}}{\sum_{t=1}^{T} W_{HP,t}} \quad (6)$$

where

- $Q_{HP,out,t}$ is the heat delivered to the DHN by the heat pump at time t,
- $W_{HP,t}$ is electrical input of the heat pump compressor at time t,
- $t = 1, \ldots, T$ is the index of assessed time intervals, with T being the total number of intervals.

Periods with no operation contribute zero to both sums. The auxiliary electricity (e.g., circulation or submersible pumps used for ATES charging) is excluded from $W_{HP,t}$ and treated separately in the cost and LCA calculations.

2.5. Computation of Difference in Heat Supply Composition

Based on the inputs defined in Sections 2.3 and 2.4, this section formulates and solves a merit-order dispatch LP for the reference and HT-ATES integration scenarios, yielding hourly heat-generation changes for existing technologies and HT-ATES. The alteration of heat supply composition is determined by cost-optimal dispatch of heating technologies in both the reference and integration scenarios via DH-MO. In the reference scenario, the DH-MO determines which heat providers supply how much of the demand. In the integration scenario, the HT-ATES is added, and the model re-optimizes the dispatch to meet the same demand. The difference in outputs between the two scenarios identifies which technologies reduce or increase their heat production due to HT-ATES integration. Each time, interval t is solved independently in an LP framework based on heat demand, must-run capacities, flexible capacities, and marginal costs. After each time interval t, the output and losses of HT-ATES are subtracted from its initial storage capacity until the stored heat is depleted.

Objective function: minimize the cost of flexible output:

$$\min_{\mathbf{x}_t} \mathbf{c}_{var,t}^{\top} \mathbf{x}_t \tag{7}$$

where $\mathbf{x}_{t(i\times 1)}$ is the flexible output vector in interval t, with each element $x_{i,t}$ representing the flexible output of technology i.

Constraints:

- Demand satisfaction: aggregate flexible output must equal flexible demand $x_{df,t}$:

$$\sum_{i=1}^{N} x_{i,t} = x_{df,t}. \tag{8}$$

- Definition of flexible demand:

$$x_{df,t} = \max(0, x_{d,t} - x_{run}). \tag{9}$$

- Technology limits:

$$0 \leq x_{i,t} \leq x_{flex,i,t} \; \forall \; i \in \{1, \ldots, N\}. \tag{10}$$

Output: solving the objective function returns the cost-optimal flexible output vector $\mathbf{x}_t$ for the reference scenario and $\widetilde{\mathbf{x}}_t$ (with a tilde) for the integration scenario.

The change in flexible output composition $\mathbf{\Delta x}_t$ is given by the vector difference between the two scenarios:

$$\mathbf{\Delta x}_t = \widetilde{\mathbf{x}}_t - \mathbf{x}_t. \tag{11}$$

Here, $\mathbf{\Delta x}_t = [\Delta x_{i=1,t}, \ldots, \Delta x_{i=N,t}]^{\top}$ represents the difference in flexible output for each technology at time t. This vector is used to calculate aggregate marginal cost (Section 2.6).

The individual technologies' difference $\Delta x_{i,t}$ is aggregated across all time intervals $t = 1, \ldots, T$ to obtain annual technology-specific change in output:

$$\Delta x_{i,y} = \sum_{t=1}^{T} \Delta x_{i,t}. \tag{12}$$

The resulting vector of aggregated annual change in flexible heat output composition is

$$\mathbf{\Delta x}_y = \begin{pmatrix} \Delta x_{i=1,y} \\ \Delta x_{i=2,y} \\ \vdots \\ \Delta x_{i=N,y} \end{pmatrix}. \tag{13}$$

This vector $\mathbf{\Delta x}_y$ forms the basis for assessing environmental impacts in year y (Section 2.6).

2.6. Life Cycle Inventory and Impact Assessment

The LCI and impact assessment constitute the final step of the computational workflow. This step uses the dispatch results from Section 2.5, together with the technology-specific marginal flows to quantify costs and to construct the consequential inventory and to link the short-term foreground changes to long-term background LCI datasets for environmental impact quantification.

2.6.1. Economic Impact Modeling

Aggregate marginal costs are calculated from variable operating costs. For each hour t, the aggregate marginal cost is computed as:

$$\Delta C_t = \mathbf{c}_{\text{var},t}^{\top} \mathbf{\Delta x}_t. \tag{14}$$

Summing hourly values over the discharge horizon yields the annual aggregate marginal cost:

$$\Delta C_y = \sum_{t=1}^{T} \mathbf{c}_{\text{var},t}^{\top} \mathbf{\Delta x}_t. \tag{15}$$

Charging-related costs are added separately using the hourly electricity price during operation of the submersible pump.

2.6.2. Environmental Impact Modeling

Annual environmental impacts are quantified by combining short-term foreground operational changes from the dispatch model with marginal background effects represented by consequential LCI datasets.

Short-term effects are assessed distinguishing marginal technologies and marginal data [35]. While the dispatch model identifies the technologies affected by the change (Section 2.5), the marginal technologies, the flows that vary within the affected technologies' operating ranges (Section 2.3) adhere to the marginal data. Accordingly, operational impacts are disaggregated from capital assets under the assumption that installed capacities of existing technologies remain unchanged over the assessment period [30]. Applying average inventories that include infrastructure-related burdens within the DHN would therefore not be representative for the operational change assessed here. This treatment is consistent with the distinction between variable and fixed components in economic theory [60].

Long-term marginal effects in processes beyond the DHN boundary are represented using long-term marginal datasets from the ecoinvent consequential background database, following the rationale that changes in demand lead upstream production capacity to adapt over time [30]. In practice, each technology is modeled in LCA software using marginal flows with one unit of heat provision as the reference flow. The annual change in flexible output composition $\mathbf{\Delta x}_y$, together with the electricity demand for charging, is used to construct the final demand changes incorporated into the LCI model. This hybrid treatment—short-term operational effects within the DHN boundary combined with long-

term marginal background effects—enables the representation of marginal consequences across both operation and upstream supply chains.

2.6.3. Data Quality Requirements and Evaluation

Following ISO 14040/14044 [61,62], dataset selection is guided by study-specific data quality requirements covering representativeness (temporal, geographical, and technological), completeness, consistency, and reproducibility. Candidate datasets are screened against these requirements using their metadata and supporting documentation (e.g., reference region and time period, technology description, system boundary, system modeling choices, and data sources). Datasets intended to represent marginal effects should only be accepted when their documented modeling logic is compatible with a long-term marginal interpretation.

Evaluation of results is performed in three steps. First, completeness checks ensure that all relevant marginal flows, including costs and avoided flows, are covered. Where exclusions are unavoidable, their potential influence is evaluated qualitatively and, where feasible, quantitatively. Second, robustness checks are conducted via sensitivity analysis on key model parameters and on influential background datasets; variations that affect results need to be highlighted and discussed. Third, consistency checks ensure harmonized units, reference flows, and methodological choices across datasets (e.g., consistent heat units, delivery levels of energy carriers, such as electricity voltage level and natural gas pressure level, consistent output temperature levels, consistent system boundaries and system models, including the long-term marginal interpretation), and confirm the consistent application of selected impact assessment methods.

2.7. Case Study Description

To demonstrate the computational workflow, a case study is conducted for the integration of a two-well HT-ATES system into an existing high-temperature DHN with must-run capacities in the Upper Rhine Graben, Germany. The underlying data are provided by a district heating operator and subsequently adjusted for confidentiality while maintaining realistic system characteristics.

The third-generation DHN is operated to meet an exogenous heat demand. The reference case represents the existing DHN without seasonal storage. The integration case adds HT-ATES and its charging electricity demand while keeping the heat demand and generation asset portfolio unchanged. Differences between reference and integration scenario therefore arise from the altered hourly dispatch of heat generation and electricity demand for HT-ATES charging and are translated into environmental and economic impacts.

The DHN supplies an annual heat demand of approximately 2.5 TWh, with peak and minimum loads of 900 MW and 25 MW, respectively. The network operates with upper and lower supply temperature boundaries of 125 °C and 80 °C and a return temperature of 67 °C. Six types of generation technologies are currently installed: waste-incineration combined heat and power (CHP), natural gas boilers, a data center, a RSHP, biomass CHP, and deep geothermal plants. The HT-ATES is introduced as a seventh technology.

The aquifer used for the HT-ATES is characterized by thermal-hydraulic properties representative of quaternary and tertiary formations in the Upper Rhine Graben. It has a thickness of 50 m, porosity of 25%, and a hydraulic conductivity of 0.00017 m/s. Thermal properties include a volumetric heat capacity of 2.23 MJ/(m^3·K) and a thermal conductivity of 2.5 W/(m·K) [63]. These parameters are consistent with values employed in comparable ATES modeling studies and therefore provide a representative setting for assessing HT-ATES performance [58].

During discharging operation, hot water is extracted from the HT-ATES and its heat is transferred to the DHN via a 15.93 MW heat pump. System operation is controlled automatically and transitions to an idle state whenever the hot-well supply temperature falls below the DHN's median return temperature of 67 °C. This ensures that heat extraction remains technically and economically feasible. To assess the long-term performance and thermal stabilization of the HT-ATES, the system is simulated over a 30-year period. The results from year 10 are presented here, as this period is representative of a stable, cyclical operation after the initial ground warm-up phase.

The integration is evaluated over a full operational year from 1 May 2024 to 30 April 2025. Charging takes place in summer (1 May to 30 September), while discharging occurs in winter (1 October to 30 April). The operation is strictly seasonal, with no discharging in summer and no recharging in winter, reflecting a high-temperature seasonal storage strategy.

Overall, this case study is meant to demonstrate the applicability of the proposed methodology for evaluating HT-ATES integration into an existing DHN. Rather than providing quantitative validation against measured operational data, the analysis assesses the methodological approach under realistic system conditions.

3. Results

The results section demonstrates the applicability of the proposed methodology to the case study presented in Section 2.7. Specifications of heating technologies (Section 3.1) and the dynamic DHN-HT-ATES model (Section 3.2) form the foundation for the computation of changes in heat supply composition (Section 3.3) and environmental impacts and cost implications (Section 3.4).

3.1. Case Study: Specifications of District Heating Technologies

Three of the existing technologies are considered must-run due to regulatory, economic, or operational constraints (Table 1): The waste incineration CHP [64] and biomass CHP plants [50] produce heat as a byproduct of mandatory waste processing due to disposal obligations; the deep geothermal plants operate at an aggregate minimum output of 100 MW to prevent clogging during downtime. Available and thus flexible capacity remain constant across time intervals for all technologies except HT-ATES. For this technology, the capacity is 0 MWh in the reference scenario and 15.93 MWh in the integration scenario, provided that stored heat is available; otherwise, it equals the remaining stored heat.

Table 1. Available capacities ($x_{\mathrm{av},i,t}$), must-run capacities ($x_{\mathrm{run},i}$), and flexible capacities ($x_{\mathrm{flex},i,t}$) of heating technologies ($i = 1, \ldots, 7$); *: if available.

Reference Scenario	i	$x_{\mathrm{av},i,t}$ (MWh)	$x_{\mathrm{run},i}$ (MWh)	$x_{\mathrm{flex},i,t}$ (MWh)
Waste incineration CHP	(1)	125	125	0
Gas boilers (aggregated)	(2)	440	0	440
Data center	(3)	30	0	30
RSHP (aggregated)	(4)	150	0	150
Biomass CHP	(5)	45	45	0
Deep geothermal plants	(6)	125	100	25
Total		915	270	645
Integration Scenario				
HT-ATES	(7)	15.93 *	0	15.93 *

Table 2 presents the marginal flows and their magnitude of change for a ±1 MWh variation in heat output. Natural gas boiler flows are based on the dataset "heat production, natural gas, at boiler condensing modulating >100 kW—Europe without Switzerland" from the ecoinvent 3.10 consequential database [43], with the flows "electricity" and "industrial furnace" subtracted. CO_2 emissions were updated according to stoichiometric ratios, and oxygen and water flows were added. All other activities were modeled individually. The HT-ATES process is described in detail in Section 3.2.

Table 2. Marginal flows including costs of heating technologies per MWh flexible output (η_{ng}: efficiency gas boiler; DC: data center; Riv: river source heat pump; Geo: deep geothermal; HP: heat pump; W_{SP}: electrical input submersible pump).

	Gas Boiler (Natural Gas)	**Data Center**	**RSHP**	**Deep Geothermal**	**HT-ATES**
Efficiency	η_{ng} = 98%	COP_{DC} = 3.0	$SCOP_{Riv}$ = 2.6	COP_{Geo} = 30	$SCOP_{HP,ATES}$ = 4.21
Input 1	Natural Gas (11 kWh/m^3; 0.74 kg/m^3)	Electricity	Electricity	Electricity	Electricity (Heat pump$_{ATES}$; submersible pump)
Formula	$\frac{1\ \text{MWh}\cdot\text{m}^3}{\eta_{ng}\cdot 0.011\ \text{MWh}}$	$\frac{1}{COP_{DC}}$	$\frac{1}{SCOP_{Riv}}$	$\frac{1}{COP_{Geo}}$	$\frac{1}{SCOP_{HP,ATES}} + \frac{W_{SP}}{15.93}$
Value	92.76 m^3	0.33 MWh	0.38 MWh	0.03 MWh	0.24 MWh
Input 2	O_2	Heat$_{DC}$	Heat$_{Riv}$	Heat$_{Geo}$	Heat$_{ATES}$
Formula	stoichiometric ration	$1 - \frac{1}{COP_{DC}}$	$1 - \frac{1}{SCOP_{Riv}}$	$1 - \frac{1}{COP_{Geo}}$	$1 - \frac{1}{SCOP_{HP,ATES}}$
Value	274 kg	0.67 MWh	0.62 MWh	0.97 MWh	0.76 MWh
Output 1	CO_2				
Formula	stoichiometric ration				
Value	189 kg				
Output 2	H_2O				
Formula	stoichiometric ration				
Value	154 kg				
Output 3	Further linearly scaled elementary flows from ecoinvent * dataset "heat production, natural gas, at boiler condensing modulating >100 kW—Europe without Switzerland"				
Marginal Cost	Natural gas EUAs	Electricity	Electricity	Electricity	Electricity

* ecoinvent 3.10 consequential.

Marginal costs of the technologies depend on the commodity prices of natural gas, electricity, and carbon allowances. Hourly wholesale day-ahead electricity prices are taken from Ember [65]. Natural gas prices are approximated using monthly import prices reported by Statistisches Bundesamt [66], and an average secondary market price of EUR 65.23 for 2024 is applied for European Union Allowances (EUAs) [67] to calculate time series of the technologies' marginal cost from 1 May 2024 to 30 April 2025.

3.2. Case Study: Application of Dynamic DHN-HT-ATES Model

In this study, we derive hourly heat demand data from monthly resolved historic demand values of the DHN and weather data for the case study's geographical region. The approach follows Lamaison et al. [68] using the HeatPro Python package (v0.1.5) [69]. First, the monthly demand values are combined with hourly weather data to simulate the DHN's supply and return temperatures, with predefined upper and lower supply temperature boundaries of 125 °C and 80 °C. The monthly heat demand is then disaggregated into hourly values based on the weather data to derive a quasi-dynamic hourly resolved heat demand curve (Figure 4). The maximum number of discharge hours is the winter period of $T = 5088\ (\text{h})$.

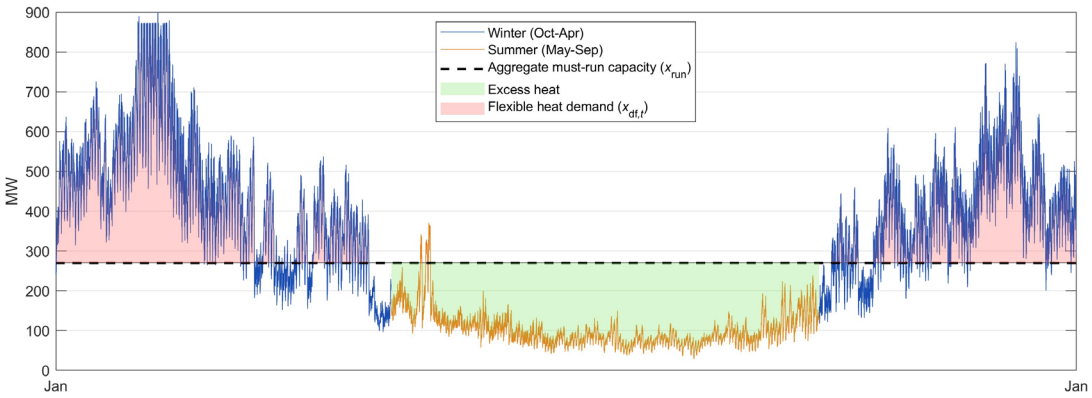


Figure 4. Quasi-dynamic heat demand curve ($\Delta t = 1$ h) for one year.

In the representative annual cycle in year 10 of operation, a quantitative assessment shows that a total of 50.71 GWh was injected into the aquifer storage, based on available surplus heat from must-run units. Following a discharge strategy unbound by merit order, the system successfully extracted 40.87 GWh with a SCOP of 4.21. This energy balance corresponds to a net thermal loss of 9.84 GWh, giving the system a round-trip thermal recovery efficiency of 80.6%. The total operational time for both charging and discharging amounted to 6983 h, which determines the average hourly thermal loss of 1.41 MWh. During the charging period from May until September, the losses are therefore calculated to 5176 MWh, leading to an available heat storage capacity of 45.53 GWh at the beginning of the discharge period. Those numbers represent the maximum technically available discharge capacity and the shortest discharge time horizon. In the merit-order schedule, the discharge time-horizon is extended through economic constraints and the discharge capacity reduced due to longer idle times, leading to higher losses.

In addition to thermal performance, the electrical energy consumption was assessed. The charging process, active in 3621 h, relied on a submersible pump with a power rating of 37.32 kW [70], resulting in a total electricity demand of 135.14 MWh.

Marginal flows of heat provision from the HT-ATES include electricity for heat pump and submersible pump operation. The submersible pump demand is divided by 15.93 to approximate the amount of electricity per MWh of heat output.

3.3. Case Study: Computation of Difference in Heat Supply Composition

The computation of differences in flexible output composition is illustrated for two representative time intervals, distinguished by the level of heat demand (Table 3). Example (1) shows a case where demand exceeds must-run capacities, while Example (2) represents a case where demand is lower than must-run capacities.

Table 3. Examples of flexible heat demand calculation for two individual time intervals.

	Example (1) $x_{d,t} > x_{run}$	**Example (2)** $x_{d,t} < x_{run}$
$x_{d,t}$	500 MWh	150 MWh
x_{run}	270 MWh	270 MWh
$x_{df,t}$	230 MWh	0 MWh

In the LP model, the demand satisfaction constraint is expressed by flexible heat demand $x_{df,t}$, derived from heat demand $x_{d,t}$ and aggregate must-run capacities x_{run}.

Technology-specific capacity limits are listed in Table 1. For the illustrative example, we assume the following hypothetical marginal costs:

$$\mathbf{c}_{\text{var},t} = \begin{bmatrix} 0 & 48.51 & 25.35 & 29.25 & 0 & 2.53 & 18.05 \end{bmatrix}^{\top}. \tag{16}$$

In Example (1), 230 MWh must be supplied by flexible technologies in both the reference scenario and the integration scenario. Deep geothermal covers 25 MWh (Table 1) as most cost-effective technology, followed by the data center with 30 MWh, RSHP with 150 MWh, and gas boilers with 25 MWh, giving a cost-optimal flexible output composition of

$$\mathbf{x}_t = \begin{bmatrix} 0 & 25 & 30 & 150 & 0 & 25 & 0 \end{bmatrix}^{\top}. \tag{17}$$

With HT-ATES integrated, the DH-MO shifts. Ranked second in the order—more costly than deep geothermal but more cost-effective than the data center—HT-ATES replaces 15.93 MWh from gas boilers, resulting in

$$\widetilde{\mathbf{x}}_t = \begin{bmatrix} 0 & 9.07 & 30 & 150 & 0 & 25 & 15.93 \end{bmatrix}^{\top}, \tag{18}$$

as shown in Figure 5.

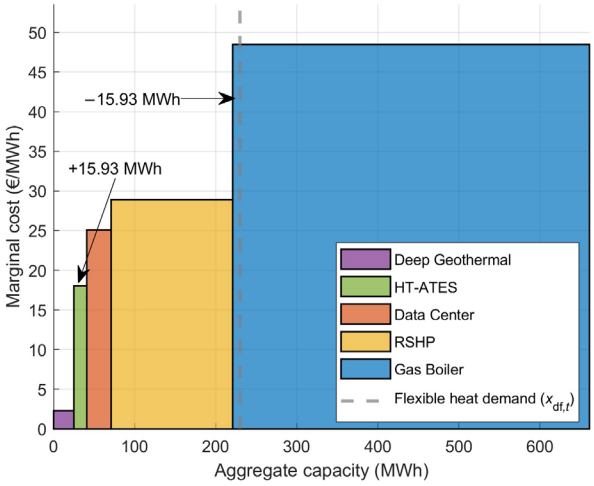


Figure 5. Change in the DH-MO due to HT-ATES integration. In the integration scenario, 15.93 MWh are provided by HT-ATES while gas boiler output is reduced by 15.93 MWh.

Thus, the difference in flexible output composition is

$$\Delta\mathbf{x}_t = \begin{bmatrix} 0 & -15.93 & 0 & 0 & 0 & 0 & 15.93 \end{bmatrix}^{\top}. \tag{19}$$

In Example (2), no flexible capacities are required; therefore, the DH-MO remains unchanged and the 120 MWh surplus must be dissipated. The difference is therefore

$$\Delta\mathbf{x}_t = \begin{bmatrix} 0 & 0 & 0 & 0 & 0 & 0 & 0 \end{bmatrix}^{\top}. \tag{20}$$

After each time interval t, the heat delivered and the heat losses from the initial stored heat are subtracted until no heat is left in the HT-ATES. Applying the LP to all winter hours with time-resolved marginal costs provides insights into the displaced technologies, the hours HT-ATES operates at full or partial load, and the duration until storage is exhausted (Figure 6). In this example, HT-ATES primarily displaces natural gas and RSHP, with only minor displacement of data centers, while deep geothermal is never displaced. The storage

is fully depleted after 4251 h, therefore 892 h later than without the consideration of merit order dispatch principles.

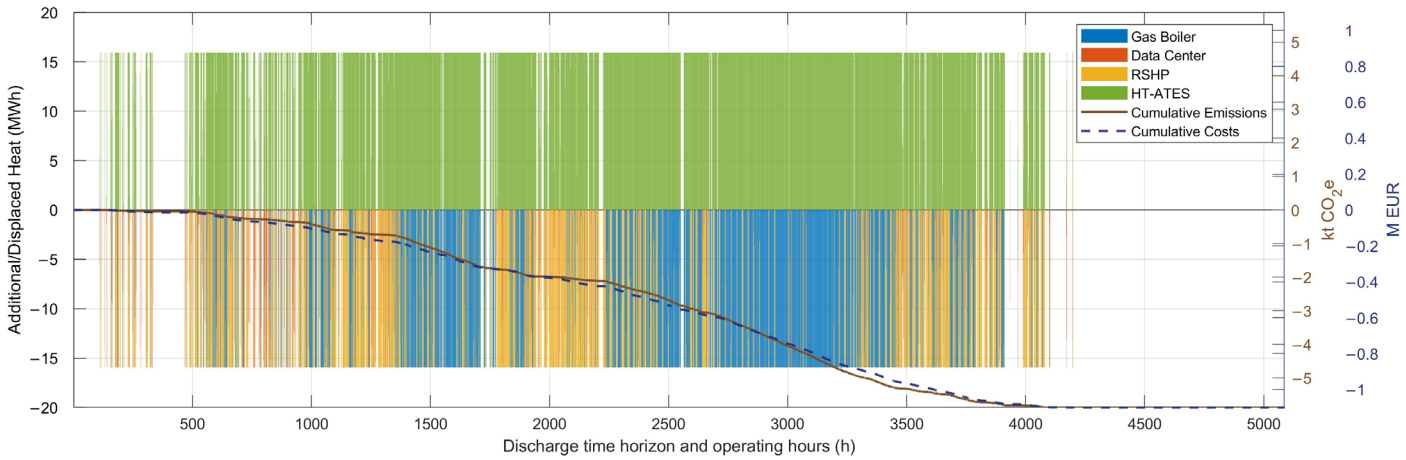


Figure 6. Time-resolved heat provided by the HT-ATES and displaced heat from existing technologies due to merit-order effects including cumulative avoided emissions and costs.

The aggregate difference in flexible output composition is obtained by summing over all time intervals, yielding

$$\sum_{t=1}^{T} \Delta \mathbf{x}_t [\text{GWh}] = \begin{bmatrix} 0 \\ -24.2 \\ -3.7 \\ -23.9 \\ 0 \\ 0 \\ +51.8 \end{bmatrix}. \quad (21)$$

Negative values indicate reduced output from existing technologies, while positive values represent additional output from HT-ATES. As defined in the demand satisfaction constraint, net changes in heat provision remain unchanged (Figure 7).

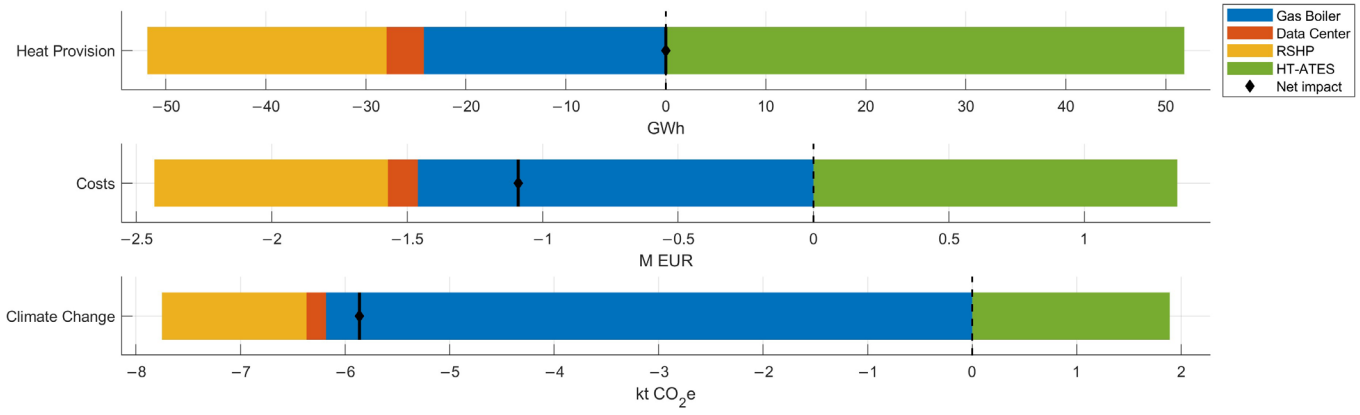


Figure 7. Contribution changes in heating technologies to (top) heat provision (GWh), (middle) total costs (M EUR), and (bottom) climate change impacts (kt CO_2e). Technologies with zero contribution across all indicators are omitted. The vertical dashed line denotes the zero reference. The black diamond indicates the net impact for each indicator (Heat: 0 GWh; Costs: EUR—1.09 M; Climate Change:—5.86 kt CO_2e).

3.4. Case Study: Life Cycle Inventory and Impact Assessment

Economic impacts are computed by multiplying hourly dispatch deltas with hourly resolved marginal costs and by aggregating results over the year including hourly costs for charging. Environmental impacts are quantified via LCI and impact assessment in the Activity Browser v2.11.2, https://github.com/LCA-ActivityBrowser/ (accessed on 5 September 2025) [71] for the case study. Heating technologies and their respective marginal data are modeled with the ecoinvent consequential 3.10 database [43]. The final demand reflects the difference in heat supply composition and the electricity demand for charging. Life cycle impacts are calculated for the impact category climate change with the indicator Global Warming Potential 100 years (GWP_{100}) using the Intergovernmental Panel on Climate Change (IPCC) 2021 method [72]. For natural gas and electricity, the following datasets are applied: market for natural gas, high pressure—DE and market for electricity, medium voltage—DE.

LCI datasets are selected to match the geographical scope (DE-Germany), the energy carrier and delivery level relevant to the foreground processes (electricity at medium voltage; natural gas at high pressure), and the long-term marginal perspective of processes outside the DHN operator's control. To test robustness against background-data for electricity, we additionally apply two prospective marginal electricity datasets (2035 and 2050) in the Section 4.

The importance of time-explicit impact calculation is illustrated in Figure 6. Cumulative avoided costs and avoided emissions increase most strongly when gas boilers are marginal and therefore primarily displaced by HT-ATES discharge, whereas the curves flatten during periods when other technologies are at the margin.

On an annual basis, aggregate net cost savings amount to EUR 1.09 M (Figure 7). This value comprises EUR 1.1 M of aggregate marginal cost savings from the changed heat supply and EUR 10 k of charging-related electricity costs. While the net heat provision remains unchanged (by computational constraints), HT-ATES reduces operational costs primarily through the reduced operation of cost-intensive gas boilers. Net climate change impacts decrease by 5.86 kt CO_2e, comprising 5.88 kt CO_2e of aggregate avoided emissions and 20 t CO_2e charging-related emissions. Consistent with the economic results, the majority of avoided emissions is associated with reduced natural gas (−6.2 kt CO_2e).

To contextualize the net results, the contribution of HT-ATES to gross (magnitude-based) contribution changes is reported. Here, "gross" refers to the sum of absolute positive (additional) and absolute negative (displaced) contributions across technologies to highlight how they offset each other. HT-ATES-related additional contributions account for 35.6% of the gross cost change and 19.6% of the gross climate change. In other words, the avoided costs and avoided climate change impacts exceed the additional contributions by factors of approximately 1.8 and 4.1, respectively.

The proposed dynamic consequential framework therefore quantifies both when (Figure 6) and through which marginal substitutions (Figure 7) HT-ATES operation yields avoided costs and reduced climate change impacts. Robustness of net results is assessed via a one-at-a-time sensitivity analysis and alternative marginal electricity datasets (Section 4.2).

4. Discussion

This discussion section compares the DH-MO operating schedule with two other operation schedules (Section 4.1), tests robustness of case study results in a sensitivity analysis (Section 4.2), and provides limitations (Section 4.3) of conceptual assumptions and computational simplifications.

4.1. Comparison with Alternative Operation Schedules

In the following, the impacts of merit-order (MO) dispatch are compared to two alternative operation schedules, namely (NG) for displacing only natural gas and (IN) for independent discharge, and their impacts on cost and climate change are assessed.

At present, HT-ATES operation is modeled to dispatch whenever it is more cost-effective than competing technologies (MO). An alternative strategy (NG) would be to restrict dispatch to displacing only the most expensive unit during peak load times, in our example the gas boiler. The calculation considers must-run technologies, and the HT-ATES only displaces natural gas. The IN-operation schedule considers the HT-ATES dispatch as in the dynamic DHN-HT-ATES model. It provides a constant amount of heat of 15.93 MWh/h until the storage is fully discharged, irrespective of demand and marginal costs. Still, only flexible technologies would be displaced, assuming heat dissipation of the HT-ATES in times where heat demand is covered by must-run capacities.

Results show that the greatest utilization of stored heat occurs in the IN schedule (Table 4). A total of 53.5 GWh is provided to the DHN, resulting in an efficiency of 80.6% (see Section 3.2) and the shortest duration until storage depletion (3359 h). Displacing only natural gas results in a low efficiency of 40.2%; due to the limited time, natural gas is used. Direct HT-ATES costs are lowest in the NG schedule, since operating hours are few in comparison to the other operating schedule. However, the cost per MWh provided heat is EUR 7.2 higher due to an incomplete utilization of the storage, resulting in a discharge time greater than 5088 h, therefore spanning into the charging cycle. While the net cost per MWh including avoided costs has the highest magnitude in NG schedule, because it only displaced the most cost-intensive technology, total net cost savings in the MO schedule are about EUR 370 k higher.

Table 4. Comparison of different operation schedules of the HT-ATES. Best performing schedules in performance and impact categories are highlighted in bold.

	HT-ATES Heat Provided to DHN [GWh]	Heat Extracted [GWh] (Efficiency * [%])	Discharge Time Horizon [h] (Discharge Operating Hours [h])	Direct HT-ATES Cost [M EUR] (per HT-ATES Heat Provided to DHN [EUR/MWh])	Net Cost DHN [M EUR] (per HT-ATES Heat Provided to DHN [EUR/MWh])	Direct HT-ATES Climate Change [kt CO_2e] (per HT-ATES Heat Provided to DHN [kg CO_2e/MWh])	Net Climate Change DHN [kt CO_2e] (per HT-ATES Heat Provided to DHN [kg CO_2e/MWh])
MO	51.8	39.5 (77.9)	4251 (3299)	1.34 **(25.9)**	**−1.09** (−21.0)	1.89 (36.4)	**−5.86** (−113)
NG	26.7	20.4 (40.2)	5088→ (1759)	**0.88** (33.1)	−0.72 **(−27.0)**	**0.98** (36.8)	−5.84 **(−219)**
IN	**53.5**	**40.9 (80.6)**	3359 (3359)	1.39 (25.9)	−0.70 (−13.1)	1.95 **(36.4)**	−4.99 (−93)

* In relation to injected heat of 50.71 GWh.

Climate change numbers show a similar picture. While the lowest direct impacts of the HT-ATES occur in the NG schedule, due to a low number of operation hours, the IN schedule provides the lowest impacts per unit of heat provision. However, if the DHN and avoided heat is considered, MO provides the highest greenhouse gas savings in total numbers, even though the savings per MWh heat provision are highest in the NG schedule.

The findings show that alternative dispatch strategies can significantly affect the results and therefore should be evaluated considering time-dependent operation of competing technologies. The optimization objective should be carefully considered, because total net impacts might be counterintuitive to relative impacts per MWh. For example, using the NG schedule because of lowest impacts per MWh would lose EUR 370 k in total net costs compared to the MO schedule while also reducing 20 t less CO_2e than in the MO schedule.

While the results provide insights into operational impacts, it should be acknowledged that capital expenditures and system lifetimes must also be considered to inform decision-making about the technology's integration.

4.2. Sensitivity Analysis

Local robustness of net costs and net emissions is evaluated through a one-at-a-time sensitivity analysis of key parameters (Figure 8), supplemented by two alternative datasets for marginal electricity background data.

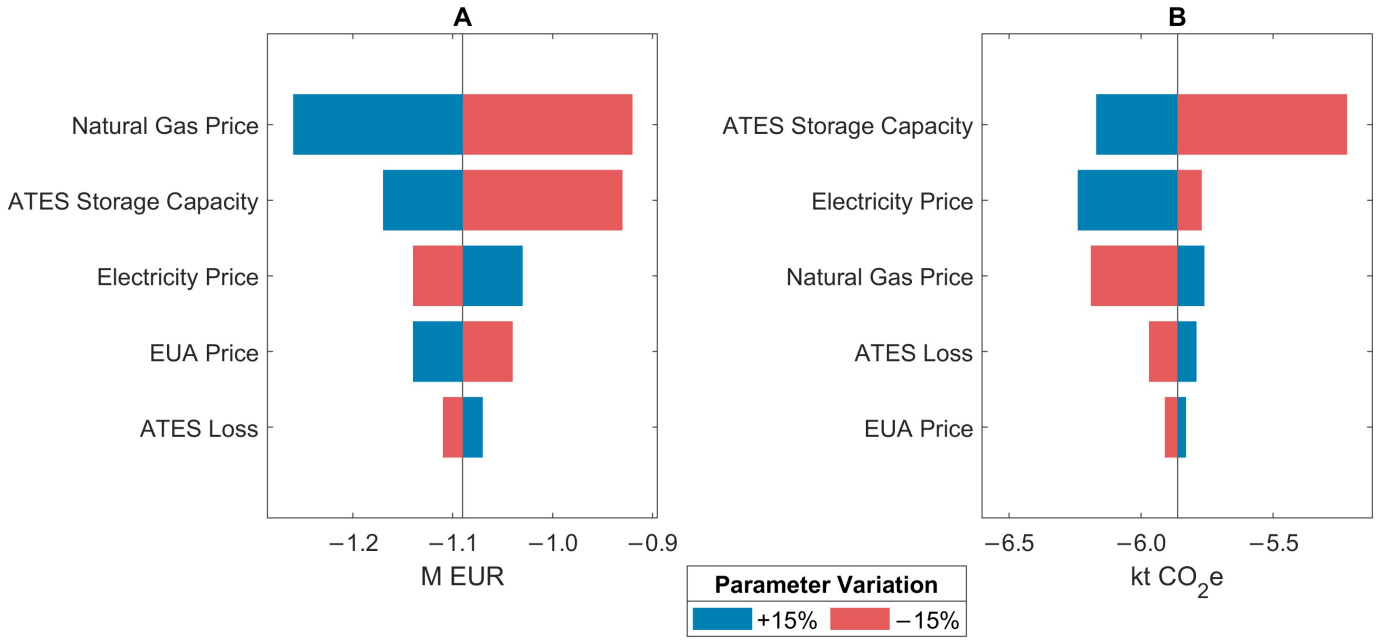


Figure 8. Sensitivity analysis of key parameters for net cost of the DHN (**A**) and net climate change impacts (**B**).

In the one-at-a-time sensitivity analysis, several parameters influence both net costs and net emissions. Increases in natural gas and EUA prices lead to larger magnitudes of avoided costs while slightly reducing avoided climate change impacts. While the increase in avoided costs associated with higher natural gas prices is intuitive, the reduction in avoided emissions can be explained by shifts in the merit order. As natural gas becomes more expensive, gas boilers are more frequently idle, resulting in the displacement of alternative technologies instead. In the case study, these displaced technologies exhibit lower environmental impacts, which reduces the overall magnitude of avoided emissions. By contrast, higher electricity prices decrease the magnitude of avoided costs but increase avoided climate change impacts. Although higher electricity prices increase the magnitude of displaced heat costs, these gains are offset by higher operating costs of the HT-ATES, leading to lower net avoided costs. At the same time, higher electricity prices cause gas boilers to be displaced more frequently, thereby increasing magnitude of avoided emissions. Storage capacity also plays a critical role, with larger capacities improving both net costs and net emissions due to longer operation times and greater volumes of displaced heat. As expected, higher thermal losses reduce both avoided costs and avoided climate change impacts. Overall, natural gas price and storage capacity emerge as the most influential parameters for net DHN costs, while electricity price and EUA price show similar but more moderate effects. For climate change impacts, storage capacity is the dominant driver, with electricity and natural gas prices contributing approximately half as much to overall sensitivity.

For the assessment of alternative electricity datasets, two prospective marginal datasets for 2035 and 2050 were applied. The prospective LCIs were generated using the ScenarioLink plug-in in the Activity Browser [71], based on the premise framework [73]. This approach modifies the ecoinvent database using projections from Integrated Assessment Models (IAMs) for different years. To construct the marginal electricity datasets for Germany, the REMIND IAM [74] was used in combination with the SSP2-NPi scenario, representing a middle-of-the-road Shared Socioeconomic Pathway (SSP) with National Policies implemented (NPi) [75]. The resulting net climate change impacts show only minor deviations between the scenarios: the 2035 dataset yields avoided emissions of −5.00 kt CO_2e, while the 2050 dataset results in −4.97 kt CO_2e (Figure 9). This limited variation can be attributed to the relative robustness of long-term marginal impacts. Although average emissions and electricity mixes may change substantially over time, marginal electricity supply reflects future capacity additions, which are expected to follow similar development pathways to those observed today. While the comparison of alternative datasets provides an illustrative indication of the robustness of background data assumptions, it does not constitute a comprehensive scenario analysis. Such an analysis would require consistent, cross-parameter changes in the foreground system as well as prospective cost structures, which is identified as a direction for future research.

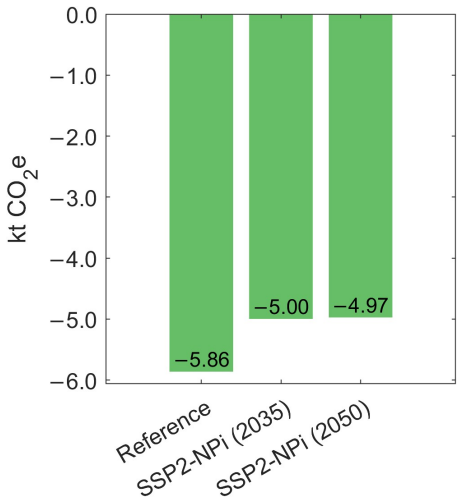


Figure 9. Net climate change impacts using three marginal electricity mix datasets for Germany: Reference, 2035, and 2050 (REMIND SSP2-NPi).

4.3. Limitations

The proposed approach provides a workflow for evaluating the integration of HT-ATES into existing DHNs, but its applicability is limited by several simplifying assumptions and methodological choices. These limitations are discussed below, alongside opportunities for future refinement.

4.3.1. Conceptual Assumptions

The framework currently allows the evaluation of the integration of a single new technology against a reference scenario, though it could also be extended to multiple additions or full replacement cases. A full LCA and cost analysis, encompassing construction, operation, and decommissioning, would be required to provide comprehensive policy guidance.

Economically, the model assumes that introducing the HT-ATES does not affect tariffs or market dynamics. While this aligns with the rationale that cost-saving technologies increase value added of the operator under fixed tariffs, it overlooks potential demand

elasticity and the possibility of consumers switching to or from individual heating, thereby affecting heat demand.

The model focuses on cost-optimal dispatch and does not explicitly target environmental or equity objectives, although the objective function could be adapted to minimize environmental impacts.

The proposed framework combines explicit short-term marginal operational modeling in the foreground system with long-term marginal representations of upstream electricity and natural gas supply. While this hybrid approach captures key components of the complex marginal effect in consequential LCA, short-term marginal responses in background supply chains are not represented explicitly. Modeling short-term consequences in the background system requires a short-term consequential background database not available today.

Finally, HT-ATES is modeled as a fully flexible technology without must-run capacity. If must-run capacities were considered, aggregate must-run capacity would shift, requiring identification of the marginal cost of must-run technologies.

4.3.2. Computational Simplifications

The Modelica-based DHN–HT-ATES model is not optimized for operational control; discharge from the ATES is triggered by simple rule-based logic and is not co-optimized with the heat pump's operation. As a result, potentially beneficial control decisions, such as coordinating discharge timing with network return temperatures, adjusting pump mass flow, or adapting heat-pump setpoints to exploit COP variations with source/sink temperatures, are not captured. This simplification may overstate losses or understate achievable efficiency (e.g., SCOP) during discharge.

The ATES representation in this framework is based on a low-order thermal model, which simplifies subsurface processes to improve tractability [57]. While this approach captures key dynamics such as storage temperature evolution and heat losses, it does not fully represent complex hydrogeological processes including heterogeneity, groundwater flow variations, thermal dispersion, or chemical interactions. As a result, local site-specific effects may be underrepresented, and the model should be regarded as a system-level approximation rather than a detailed hydrogeological simulation.

The operational model employs an LP framework to optimize dispatch decisions, prioritizing computational efficiency and transparency over detailed operational realism. By assuming continuous operation and linear cost functions, the model does not represent non-linear effects such as part-load efficiency losses, minimum up- and downtime constraints, or start-up and shut-down costs. Capturing these characteristics requires mixed-integer linear programming or a non-linear program formulation in a more advanced energy system modeling environment. As a result, the LP formulation may overestimate operational flexibility and underrepresent part-load limitations, which can influence absolute results.

The LP model is solved at an hourly resolution for heat demand and supply. While this level of detail is adequate to capture intra-day and seasonal patterns and the marginal substitution effects central to this study, it does not represent faster intra-hour dynamics such as ramping constraints or start-up delays. These choices reflect an intentional trade-off between operational detail and the primary objective of the work: establishing a transparent and replicable framework that links time-resolved dispatch modeling with marginal economic and environmental life cycle data. Demand satisfaction is enforced as an equality constraint, preventing oversupply. This avoids unrealistic profiles that could violate network temperature limits but excludes cases where oversupply could be economically rational, such as under negative electricity prices.

Heat output is restricted to non-negative values, excluding cooling technologies or short-term storage cycles. In the current setup, HT-ATES discharge is modeled as a unidirectional flexible source with time-dependent storage losses, while charging is represented as a static summer redirection of excess heat rather than an optimized decision variable. This simplification may misrepresent systems with intra-seasonal charging cycles.

Finally, the LP model solves each hour independently but accounts for heat losses and evolving storage capacity. Merging the merit-order with the dynamic DHN-HT-ATES model would replace the stepwise procedure by embedding technical and economic constraints firsthand.

4.3.3. Applicability Boundaries and Transferability to Other DHNs

The quantitative results of this case study are not directly transferable to other DHNs because technology portfolios, geological conditions, and cost structures are highly site-specific. The framework itself, linking a dynamic LP-based DHN dispatch model with marginal LCA, is, however, transferable under certain conditions. To apply it to another DHN, the boundary conditions of the network must be adapted, including the heat demand profile, supply and return temperatures, and the set of available generation technologies and their installed capacities.

The DH-MO representation has to be updated to the local technology mix, efficiencies, and cost and fuel price assumptions. Within one country, cost structures for the same energy carriers may remain similar, but they require revision when different fuels are used or when a different market context is considered. The DHN-HT-ATES model likewise needs to be recalibrated to the geological and technical characteristics of the subsurface and the network (e.g., available surplus heat, operating temperature range, and injection and extraction constraints) and then reintegrated into the dynamic LP model.

In parallel, the marginal LCI datasets must be aligned with the energy carriers and technologies in the new DHN. For prospective applications, both cost assumptions and marginal LCI data should be adapted consistently with the chosen scenario framework (e.g., future energy prices and background LCI projections).

5. Conclusions

This work developed and demonstrated a consequential, operation-phase framework to quantify the marginal environmental and economic impacts of integrating HT-ATES into DHNs. By explicitly representing dispatch dynamics and time-resolved marginal substitution among multiple heat providers, the framework addresses a central limitation of prior ATES LCA research: the environmental–economic impacts of HT-ATES operation within interconnected DHNs have remained unclear because marginal displacement effects were not captured. Methodologically, the framework expands system boundaries from the storage technology to the DHN and applies a heating-system-wide functional unit to enable consistent comparison of heat supply composition changes relative to a reference system. It further links a dynamic DHN-HT-ATES model with an hourly merit-order dispatch formulation to identify time-dependent marginally displaced heat supply and the associated cost and emission variations, complemented by a hybrid assessment of short-term operational and environmental long-term effects.

Applied to an existing DHN in Germany, the results show that operational impacts are dominated by avoided heat production in marginal technologies. In the analyzed case, avoided technologies offset the direct operational impacts of HT-ATES (1.89 kt CO_2e; EUR 1.34 M) by a factor of 4.1 for climate change and 1.8 for costs. The results are highly sensitive to operational strategy: alternative schedules significantly change both net costs and emissions, and selecting schedules solely based on the best relative impact performance may

result in an untapped potential of up to EUR 370 k and 20 t CO_2e per year. Sensitivity analysis identifies storage capacity and natural gas price as dominant drivers; higher natural gas and EUA prices increase avoided costs while reducing avoided emissions, whereas higher electricity prices can erode cost benefits through increased HT-ATES operating impacts.

These findings show that robust environmental–economic conclusions for HT-ATES primarily depend on the DH-MO, which is shaped by the existing technology portfolio, market conditions, and storage performance, and therefore on the resulting time-resolved marginal displacement. Accordingly, absolute results should not be transferred without case-specific re-parameterization. The main value of the proposed approach is therefore its ability to produce decision-relevant, system-consistent net impact assessments for a given DHN by linking operational dispatch and marginal life cycle inventory (LCI) data.

Several limitations remain. The operational dispatch is represented via an LP formulation for being consistent with linear LCI data, which, however, underrepresents unit-commitment phenomena such as part-load efficiency, start-up costs, and minimum up/down times. In addition, the current hybrid impact modeling captures long-term effects primarily in the environmental background model; long-term economic feedbacks (e.g., market behavior and investment responses) are not explicitly modeled.

Future work should prioritize methodological extensions that improve operational realism while maintaining consistency with consequential inventory data. First, the dispatch model could be extended toward mixed-integer or non-linear representations to capture the unit-commitment phenomena. In parallel, this would require the development of performance-dependent marginal LCI data (e.g., inventories differentiated by load level) to avoid methodological inconsistency. This extension also raises a practical trade-off: to what extent does added operational detail improve the precision of environmental results, and at what computational and data collection cost? Second, the framework should implement bi-directional coupling between the dynamic DHN-HT-ATES model and the dispatch model to capture feedbacks between operating decisions, storage thermodynamics, and network constraints. Building on this, embedding the coupled representation in a broader multi-energy system model would enable assessment of interactions with sector-coupling technologies. Third, the hybrid impact modeling should be complemented with an explicit representation of long-term economic mechanisms (e.g., coupling to partial-equilibrium market models) to quantify market behavior, investment responses, and economy-wide cost effects alongside long-term environmental impacts.

In addition, further work should expand the framework's decision-support scope and strengthen external validity. Systematic cross-case application across DHN archetypes and geological classes, combined with uncertainty quantification and empirical validation against measured operational data, would improve generalizability and credibility. Beyond climate change and aggregated costs, the framework could be extended to additional impact categories and to external-cost accounting for socio-economic appraisal of operational decisions. A cost–benefit analysis (e.g., cost–emission Pareto fronts or eco-efficiency analyses) would allow a multi-objective optimization. Finally, prospective application should be implemented through scenario parameterization of alternative heat supply technologies and consistent prospective LCI and cost datasets, enabling forward-looking assessment of HT-ATES value under future DHN configurations, time-varying market conditions, and policy instruments.

Overall, this study provides a replicable basis for consequential, system-level assessment of HT-ATES operation in DHNs. It supports more robust decision-making on thermal storage deployment by translating marginal displacement effects into net environmental and economic consequences, thereby supporting more informed and sustainable design of low-carbon heating infrastructure.

Author Contributions: Conceptualization, N.S.; methodology, N.S. and M.O.; software, N.S. and M.O.; validation, N.S. and M.O.; formal analysis, N.S. and M.O.; investigation, N.S. and M.O.; resources, N.S. and M.O.; data curation, N.S. and M.O.; writing—original draft preparation, N.S. and M.O.; writing—review and editing, N.S., M.O. and V.Z.; visualization, N.S.; supervision, I.S., L.S. and V.Z.; project administration, I.S.; funding acquisition, I.S. and L.S. All authors have read and agreed to the published version of the manuscript.

Funding: This work was supported by the Federal Ministry of Education and Research (BMBF) Germany, project administrator Jülich, under the funding code 03G0913B for the project PotAMMO, comprising the concept development and implementation of ATES for two sites in Germany (Offenbach and Mannheim).

Data Availability Statement: The original contributions presented in this study are included in the article. Further inquiries can be directed to the corresponding author.

Acknowledgments: We thank Jens Schmugge and Clemens Rohde for their valuable discussions on energy systems modeling. During the preparation of this manuscript, the authors used ChatGPT (OpenAI, GPT-5.2 model) for the purposes of language editing and text refinement. The authors have reviewed and edited the output and take full responsibility for the content of this publication.

Conflicts of Interest: The authors declare no conflicts of interest. The funders had no role in the design of the study; in the collection, analyses, or interpretation of data; in the writing of the manuscript; or in the decision to publish the results.

Abbreviations

The following abbreviations are used in this manuscript:

ATES	Aquifer Thermal Energy Storage
CHP	Combined Heat and Power
COP	Coefficient of Performance
DE	Deutschland (Germany) in ecoinvent dataset
DH-MO	District Heating Merit Order
DHN	District Heating Network
EUA	European Allowance
GWP_{100}	Global Warming Potential 100 Years
HT-ATES	High-Temperature Aquifer Thermal Energy Storage
IAM	Integrated Assessment Model
IN	Independent Discharge Schedule
IPCC	Intergovernmental Panel on Climate Change
LCA	Life Cycle Assessment
LCI	Life Cycle Inventory
LP	Linear Program
LT-ATES	Low-Temperature Aquifer Thermal Energy Storage
MO	Merit-Order Operation Schedule
NG	Natural Gas Operation Schedule
NPi	National Policies implemented
RSHP	River Source Heat Pump
SCOP	Seasonal Coefficient of Performance
SSP	Shared Socioeconomic Pathway

Nomenclature

Indices/Subscripts

i	index of heating technology
t	index of time interval
y	index of year
N	total number of heating technologies
T	total number of assessed time intervals

~	accent for variables in integration scenario
Scalars	
$c_{i,t}$	marginal cost of technology i at time t [EUR/MWh]
$Q_{\mathrm{HP,out},t}$	heat delivered to the DHN by the heat pump at time t [MWh]
$W_{\mathrm{HP},t}$	electrical input of the heat pump compressor at time t [MWh]
W_{SP}	electrical input submersible pump [MWh]
$x_{\mathrm{av},i,t}$	available capacity of technology i at time t [MWh]
$x_{\mathrm{d},t}$	heat demand at time t [MWh]
$x_{\mathrm{df},t}$	flexible heat demand at time t [MWh]
$x_{\mathrm{flex},t}$	aggregate flexible capacity at time t [MWh]
$x_{\mathrm{flex},i,t}$	flexible capacity of technology i at time t [MWh]
x_{run}	aggregate must-run capacity [MWh]
$x_{\mathrm{run},i}$	must-run capacity of technology i [MWh]
x_t	aggregate flexible output at time t [MWh]
$x_{i,t}$	flexible output of technology i at time t [MWh]
$P_{i,t}$	available heating power of technology i at time t [MW]
ΔC_t	aggregate marginal cost at time t [EUR]
ΔC_y	annual aggregate marginal cost [EUR]
$\Delta Electricity$	marginal change of electricity [MWh]
$\Delta Q_{\mathrm{river}}$	marginal change of heat from river [MWh]
ΔQ_{DH}	marginal change of a heat demand in district heating network [MWh]
Δt	duration of time interval considered in the analysis [h]
$\Delta x_{i,t}$	flexible output difference of technology i at time t [MWh]
$\Delta x_{i,y}$	aggregate flexible output difference of technology i in year y [MWh]
Vectors	
$\mathbf{c}_{\mathrm{var},t}$	marginal cost vector at time t, $(i \times 1)$
$\mathbf{x}_t$	flexible output vector at time t, $(i \times 1)$
$\mathbf{\Delta x}_t$	difference vector of flexible output composition at time t, $(i \times 1)$
$\mathbf{\Delta x}_y$	aggregate difference of flexible output composition in year y, $(i \times 1)$

References

1. Autelitano, K.; Famiglietti, J.; Aprile, M.; Motta, M. Towards Life Cycle Assessment for the Environmental Evaluation of District Heating and Cooling: A Critical Review. *Standards* **2024**, *4*, 102–132. [CrossRef]
2. Tien, P.W.; Wang, H.; Tokbolat, S.; Boukhanouf, R.; Calautit, J.; Darkwa, J. Application of life cycle assessment for enhancing sustainability of district heating: A multi-level approach. *Energy Rep.* **2025**, *13*, 5077–5096. [CrossRef]
3. Stemmle, R.; Arab, A.; Bauer, S.; Beyer, C.; Blöcher, G.; Bossennec, C.; Dörnbrack, M.; Hahn, F.; Jaeger, P.; Kranz, S.; et al. Current research on aquifer thermal energy storage (ATES) in Germany. *Grund. Z. Fachsekt. Hydrogeol.* **2025**, *30*, 107–124. [CrossRef]
4. Moser, S.; Puschnigg, S.; Rodin, V. Designing the Heat Merit Order to determine the value of industrial waste heat for district heating systems. *Energy* **2020**, *200*, 117579. [CrossRef]
5. Fleuchaus, P.; Godschalk, B.; Stober, I.; Blum, P. Worldwide application of aquifer thermal energy storage—A review. *Renew. Sustain. Energy Rev.* **2018**, *94*, 861–876. [CrossRef]
6. Hoekstra, N.; Pellegrini, M.; Bloemendal, M.; Spaak, G.; Gallego, A.A.; Comins, J.R.; Grotenhuis, T.; Picone, S.; Murrell, A.; Steeman, H.; et al. Increasing market opportunities for renewable energy technologies with innovations in aquifer thermal energy storage. *Sci. Total Environ.* **2020**, *709*, 136142. [CrossRef]
7. Daniilidis, A.; Mindel, J.E.; Filho, F.D.O.; Guglielmetti, L. Techno-economic assessment and operational CO_2 emissions of High-Temperature Aquifer Thermal Energy Storage (HT-ATES) using demand-driven and subsurface-constrained dimensioning. *Energy* **2022**, *249*, 123682. [CrossRef]
8. Figueira, J.S.; Gil, A.G.; Vieira, A.; Michopoulos, A.K.; Boon, D.P.; Loveridge, F.; Cecinato, F.; Götzl, G.; Epting, J.; Zosseder, K.; et al. Shallow geothermal energy systems for district heating and cooling networks: Review and technological progression through case studies. *Renew. Energy* **2024**, *236*, 121436. [CrossRef]
9. Todorov, O.; Alanne, K.; Virtanen, M.; Kosonen, R. Aquifer Thermal Energy Storage (ATES) for District Heating and Cooling: A Novel Modeling Approach Applied in a Case Study of a Finnish Urban District. *Energies* **2020**, *13*, 2478. [CrossRef]
10. Marojević, K.; Kurevija, T.; Macenić, M. Challenges and Opportunities for Aquifer Thermal Energy Storage (ATES) in EU Energy Transition Efforts—An Overview. *Energies* **2025**, *18*, 1001. [CrossRef]

11. Stemmle, R.; Hanna, R.; Menberg, K.; Østergaard, P.A.; Jackson, M.; Staffell, I.; Blum, P. Policies for aquifer thermal energy storage: International comparison, barriers and recommendations. *Clean Technol. Environ. Policy* **2025**, *27*, 1455–1478. [CrossRef]
12. Zeghici, R.M.; Oude Essink, G.H.; Hartog, N.; Sommer, W. Integrated assessment of variable density–viscosity groundwater flow for a high temperature mono-well aquifer thermal energy storage (HT-ATES) system in a geothermal reservoir. *Geothermics* **2015**, *55*, 58–68. [CrossRef]
13. Pallotta, G.; Marrasso, E.; Martone, C.; Luciano, N.; Squarzoni, G.; Roselli, C.; Sasso, M. Aquifer thermal energy storage for decarbonising heating and cooling energy supply in southern Europe: A dynamic environmental impact assessment. *Appl. Energy* **2025**, *394*, 126105. [CrossRef]
14. Agate, G.; Colucci, F.; Luciano, N.; Marrasso, E.; Martone, C.; Pallotta, G.; Roselli, C.; Sasso, M.; Squarzoni, G. Multi-software based dynamic modelling of a water-to-water heat pump interacting with an aquifer thermal energy storage system. *Renew. Energy* **2024**, *237*, 121795. [CrossRef]
15. Lüchinger, R.; Hendry, R.; Walter, H.; Worlitschek, J.; Schuetz, P. Cost Analysis for Large Thermal Energy Storage Systems. *ASME J. Eng. Sustain. Build. Cities* **2025**, *6*, 021006. [CrossRef]
16. Godinaud, J.; Loubet, P.; Gombert-Courvoisier, S.; Pryet, A.; Dupuy, A.; Larroque, F. Life Cycle Assessment of an Aquifer Thermal Energy Storage System: Influence of design parameters and comparison with conventional systems. *Geothermics* **2024**, *120*, 102996. [CrossRef]
17. Ni, Z.; Wang, Y.; Wang, Y.; Chen, S.; Xie, M.; Grotenhuis, T.; Qiu, R. Comparative Life-Cycle Assessment of Aquifer Thermal Energy Storage Integrated with in Situ Bioremediation of Chlorinated Volatile Organic Compounds. *Environ. Sci. Technol.* **2020**, *54*, 3039–3049. [CrossRef] [PubMed]
18. Moulopoulos, A. Life Cycle Assessment of an Aquifer Thermal Energy Storage system: Exploring the Environmental Performance of Shallow Subsurface Space Development. Master's Thesis, Utrecht University, Utrecht, The Netherlands, 2014.
19. Tomasetta, C.; van Ree, C.C.D.F.; Griffioen, J. Life Cycle Analysis of Underground Thermal Energy Storage. In *Engineering Geology for Society and Territory—Volume 5: Urban Geology, Sustainable Planning and Landscape Exploitation*; Lollino, G., Manconi, A., Guzzetti, F., Culshaw, M., Bobrowsky, P., Luino, F., Eds.; Springer International Publishing: Cham, Switzerland, 2015; pp. 1213–1217. [CrossRef]
20. Stemmle, R.; Blum, P.; Schüppler, S.; Fleuchaus, P.; Limoges, M.; Bayer, P.; Menberg, K. Environmental impacts of aquifer thermal energy storage (ATES). *Renew. Sustain. Energy Rev.* **2021**, *151*, 111560. [CrossRef]
21. Tomasetta, C. Life Cycle Assessement of Underground Thermal Energy Storage Systems: Aquifer Thermal Energy Storage versus Borehole Thermal Energy Storage. Master's Thesis, Università Ca' Foscari, Venice, Italy, 2013.
22. Werner, J. Environmental Footprint of High Temperature Aquifer Thermal Energy Storage. Master's Thesis, Utrecht University, Utrecht, The Netherlands, 2016.
23. Weise, J.; Bott, C.; Menberg, K.; Bayer, P. Comprehensive life cycle assessment of selected seasonal thermal energy storage systems. *Renew. Energy* **2026**, *256*, 124232. [CrossRef]
24. Scholliers, N.; Ohagen, M.; Bossennec, C.; Sass, I.; Zeller, V.; Schebek, L. Identification of key factors for the sustainable integration of high-temperature aquifer thermal energy storage systems in district heating networks. *Smart Energy* **2024**, *13*, 100134. [CrossRef]
25. Drijver, B.; van Aarssen, M.; Zwart, B.D. High-temperature aquifer thermal energy storage (HT-ATES): Sustainable and multi-usable. In Proceedings of the Innostock 2012—The 12th International Conference on Energy Storage, Lleida, Catalonia, Spain, 16–18 May 2012.
26. Schüppler, S.; Fleuchaus, P.; Blum, P. Techno-economic and environmental analysis of an Aquifer Thermal Energy Storage (ATES) in Germany. *Geotherm Energy* **2019**, *7*, 11. [CrossRef]
27. Fleuchaus, P.; Schüppler, S.; Bloemendal, M.; Guglielmetti, L.; Opel, O.; Blum, P. Risk analysis of High-Temperature Aquifer Thermal Energy Storage (HT-ATES). *Renew. Sustain. Energy Rev.* **2020**, *133*, 110153. [CrossRef]
28. Frederiksen, S.; Werner, S. *District Heating and Cooling*; Studentlitteratur AB: Lund, Sweden, 2013.
29. Ohagen, M.; Koch, M.; Scholliers, N.; Pham, H.T.; Holler, J.K.; Sass, I. Managing High Groundwater Velocities in Aquifer Thermal Energy Storage Systems: A Three-Well Conceptual Model. *Energies* **2025**, *18*, 4308. [CrossRef]
30. Ekvall, T. Attributional and Consequential Life Cycle Assessment. In *Sustainability Assessment at the 21st Century*; José Bastante-Ceca, M., Luis Fuentes-Bargues, J., Hufnagel, L., Mihai, F.-C., Iatu, C., Eds.; IntechOpen: London, UK, 2020. [CrossRef]
31. Finnveden, G.; Hauschild, M.Z.; Ekvall, T.; Guinée, J.B.; Heijungs, R.; Hellweg, S.; Koehler, A.; Pennington, D.; Suh, S. Recent developments in Life Cycle Assessment. *J. Environ. Manag.* **2009**, *91*, 1–21. [CrossRef] [PubMed]
32. Vanhoudt, D.; Desmedt, J.; van Bael, J.; Robeyn, N.; Hoes, H. An aquifer thermal storage system in a Belgian hospital: Long-term experimental evaluation of energy and cost savings. *Energy Build.* **2011**, *43*, 3657–3665. [CrossRef]
33. Ghaebi, H.; Bahadori, M.N.; Saidi, M.H. Economic and Environmental Evaluations of Different Operation Alternatives of an Aquifer Thermal Energy Storage in Tehran, Iran. *Sci. Iran.* **2017**, *24*, 610–623. [CrossRef]
34. Plevin, R.J.; Delucchi, M.A.; Creutzig, F. Using Attributional Life Cycle Assessment to Estimate Climate-Change Mitigation Benefits Misleads Policy Makers. *J. Ind. Ecol.* **2014**, *18*, 73–83. [CrossRef]

35. Heijungs, R. Marginal and average considerations in LCA and their role for defining emission factors and characterization factors. *Int. J. Life Cycle Assess.* **2025**, *30*, 525–542. [CrossRef]
36. Zhou, D.; Li, K.; Gao, H.; Tatomir, A.; Sauter, M.; Ganzer, L. Techno-economic assessment of high-temperature aquifer thermal energy storage system, insights from a study case in Burgwedel, Germany. *Appl. Energy* **2024**, *372*, 123783. [CrossRef]
37. Remmelts, J.; Tensen, S.C.; Infante Ferreira, C.A. Seasonal thermal energy storage for large scale district heating. In Proceedings of the 13th IEA Heat Pump Conference, Jeju, Republic of Korea, 26–29 April 2021; Heat Pump Centre c/o RISE Research Institutes of Sweden: Borås, Sweden, 2021; pp. 1633–1643.
38. Réveillère, A.; Hamm, V.; Lesueur, H.; Cordier, E.; Goblet, P. Geothermal contribution to the energy mix of a heating network when using Aquifer Thermal Energy Storage: Modeling and application to the Paris basin. *Geothermics* **2013**, *47*, 69–79. [CrossRef]
39. Opel, O.; Strodel, N.; Werner, K.F.; Geffken, J.; Tribel, A.; Ruck, W. Climate-neutral and sustainable campus Leuphana University of Lueneburg. *Energy* **2017**, *141*, 2628–2639. [CrossRef]
40. Weidema, B.P.; Pizzol, M.; Schmidt, J.; Thoma, G. Attributional or consequential Life Cycle Assessment: A matter of social responsibility. *J. Clean. Prod.* **2018**, *174*, 305–314. [CrossRef]
41. Weidema, B.P.; Frees, N.; Nielsen, A.-M. Marginal production technologies for life cycle inventories. *Int. J. Life Cycle Assess.* **1999**, *4*, 48–56. [CrossRef]
42. Eriksson, O.; Finnveden, G.; Ekvall, T.; Björklund, A. Life cycle assessment of fuels for district heating: A comparison of waste incineration, biomass- and natural gas combustion. *Energy Policy* **2007**, *35*, 1346–1362. [CrossRef]
43. Wernet, G.; Bauer, C.; Steubing, B.; Reinhard, J.; Moreno-Ruiz, E.; Weidema, B. The ecoinvent database version 3 (part I): Overview and methodology. *Int. J. Life Cycle Assess.* **2016**, *21*, 1218–1230. [CrossRef]
44. Azapagica, A.; Cliftb, R. Allocation of environmental burdens in multiple-function systems. *J. Clean. Prod.* **1999**, *7*, 101–119. [CrossRef]
45. Lund, H.; Werner, S.; Wiltshire, R.; Svendsen, S.; Thorsen, J.E.; Hvelplund, F.; Mathiesen, B.V. 4th Generation District Heating (4GDH). *Energy* **2014**, *68*, 1–11. [CrossRef]
46. Böttger, D.; Götz, M.; Theofilidi, M.; Bruckner, T. Control power provision with power-to-heat plants in systems with high shares of renewable energy sources—An illustrative analysis for Germany based on the use of electric boilers in district heating grids. *Energy* **2015**, *82*, 157–167. [CrossRef]
47. Schweiger, G.; Rantzer, J.; Ericsson, K.; Lauenburg, P. The potential of power-to-heat in Swedish district heating systems. *Energy* **2017**, *137*, 661–669. [CrossRef]
48. Volkova, A.; Reuter, S.; Puschnigg, S.; Kauko, H.; Schmidt, R.-R.; Leitner, B.; Moser, S. Cascade sub-low temperature district heating networks in existing district heating systems. *Smart Energy* **2022**, *5*, 100064. [CrossRef]
49. Kicherer, N.; Lorenzen, P.; Schäfers, H. Design of a district heating roadmap for Hamburg. *Smart Energy* **2021**, *2*, 100014. [CrossRef]
50. Schill, W.-P. Residual load, renewable surplus generation and storage requirements in Germany. *Energy Policy* **2014**, *73*, 65–79. [CrossRef]
51. Kicherer, N.; Benalcazar, P.; Lorenzen, P.; Kozlenko, O.; Tomtulu, S.; Trosdorff, J. Heat4Future: A strategic planning tool for decarbonizing district heating systems. *MethodsX* **2025**, *14*, 103222. [CrossRef] [PubMed]
52. MVV Energie AG. Flusswärmepumpe 1. 2025. Available online: https://www.mvv.de/ueber-uns/unternehmensgruppe/mvv-umwelt/aktuelle-projekte/flusswaermepumpen/flusswaermepumpe-1 (accessed on 25 October 2025).
53. Modelica: Modelica Association c/o PELAB, IDA, Linköpings Universitet. 2025. Available online: http://modelica.org/ (accessed on 30 September 2025).
54. Brück, D.; Elmqvist, H.; Mattson, S.E.; Olsson, H. Dymola for Multi-Engineering Modeling and Simulation. In Proceedings of the 2nd International Modelica Conference, Oberpfaffenhofen, Germany, 18–19 March 2002; pp. 55-1–55-8.
55. Wetter, M.; Zuo, W.; Nouidui, T.S.; Pang, X. Modelica Buildings library. *J. Build. Perform. Simul.* **2014**, *7*, 253–270. [CrossRef]
56. AIT-IES. DisHeatLib. 2022. Available online: https://github.com/AIT-IES/DisHeatLib (accessed on 30 September 2025).
57. Maccarini, A.; Wetter, M.; Varesano, D.; Bloemendal, M.; Afshari, A.; Zarrella, A. Low-order aquifer thermal energy storage model for geothermal system simulation. In Proceedings of the 15th International Modelica Conference 2023, Aachen, Germany, 9–11 October 2023; Linköping University Electronic Press: Linköping, Sweden, 2023; pp. 389–396. [CrossRef]
58. Bloemendal, M.; Olsthoorn, T. ATES systems in aquifers with high ambient groundwater flow velocity. *Geothermics* **2018**, *75*, 81–92. [CrossRef]
59. Pieper, H.; Mašatin, V.; Volkova, A.; Ommen, T.; Elmegaard, B.; Brix Markussen, W. Modelling framework for integration of large-scale heat pumps in district heating using low-temperature heat sources. *Int. J. Sustain. Energy Plan. Manag.* **2019**, *20*, 67–86. [CrossRef]
60. Mankiw, N.G. *Principles of Economics*; Cengage: Boston, MA, USA, 2021.
61. *ISO 14040:2006*; Environmental Management—Life Cycle Assessment—Principles and Framework. The International Organization for Standardization (ISO): Geneva, Switzerland, 2006.

62. *ISO 14044:2006*; Environmental Management—Life Cycle Assessment—Requirements and Guidelines. The International Organization for Standardization (ISO): Geneva, Switzerland, 2006.
63. Wirsing, G.; Luz, A. *Hydrogeologischer Bau und Aquifereigenschaften der Lockergesteine im Oberrheingraben (Baden-Württemberg)*; Regierungspräsidium Freiburg: Freiburg im Breisgau, Germany, 2007.
64. Brunner, P.H.; Rechberger, H. Waste to energy—Key element for sustainable waste management. *Waste Manag.* **2015**, *37*, 3–12. [CrossRef]
65. Ember. European Wholesale Electricity Price Data: Germany, Hourly. 2025. Available online: https://ember-energy.org/data/european-wholesale-electricity-price-data/ (accessed on 8 September 2025).
66. Statistisches Bundesamt (Destatis). Monthly Natural Gas Imports. 2025. Available online: https://www.destatis.de/EN/Themes/Economy/Foreign-Trade/Tables/natural-gas-monthly.html (accessed on 8 September 2025).
67. International Carbon Action Partnership (ICAP). *EU Emissions Trading System (EU ETS): Factsheet*; International Carbon Action Partnership (ICAP): Berlin, Germany, 2024.
68. Lamaison, N.; Collette, S.; Vallée, M.; Bavière, R. Storage influence in a combined biomass and power-to-heat district heating production plant. *Energy* **2019**, *186*, 115714. [CrossRef]
69. Beaucour, R.; Wissocq, T.; Lamaison, N. HeatPro Python Package: Generate Heat Demand Load Profile for District Heating. 2024. Available online: https://github.com/CEA-Liten/heatpro (accessed on 10 July 2025).
70. Grundfos Holding A/S. Submersible Groundwater Pumps: SP 215-2A—No. 18A356A2. 2024. Available online: https://product-selection.grundfos.com/products/sp-sp-g/sp/sp-215-2a-18A356A2 (accessed on 19 December 2024).
71. Steubing, B.; de Koning, D.; Haas, A.; Mutel, C.L. The Activity Browser—An open source LCA software building on top of the brightway framework. *Softw. Impacts* **2020**, *3*, 100012. [CrossRef]
72. Smith, C.; Nicholls, Z.; Armour, K.; Collins, W.; Forster, P.; Meinshausen, M.; Palmer, M.; Watanabe, M. The Earth's Energy Budget, Climate Feedbacks, and Climate Sensitivity Supplementary Material. In *Climate Change 2021: The Physical Science Basis: Contribution of Working Group I to the Sixth Assessment Report of the Intergovernmental Panel on Climate Change*; Masson-Delmotte, V., Zhai, P., Pirani, A., Connors, S., Péan, C., Berger, S., Caud, N., Chen, Y., Goldfarb, L., Gomis, M., et al., Eds.; Cambridge University Press: Cambridge, UK, 2021.
73. Sacchi, R.; Terlouw, T.; Siala, K.; Dirnaichner, A.; Bauer, C.; Cox, B.; Mutel, C.; Daioglou, V.; Luderer, G. PRospective EnvironMental Impact asSEment (premise): A streamlined approach to producing databases for prospective life cycle assessment using integrated assessment models. *Renew. Sustain. Energy Rev.* **2022**, *160*, 112311. [CrossRef]
74. Baumstark, L.; Bauer, N.; Benke, F.; Bertram, C.; Bi, S.; Gong, C.C.; Dietrich, J.P.; Dirnaichner, A.; Giannousakis, A.; Hilaire, J.; et al. REMIND2.1: Transformation and innovation dynamics of the energy-economic system within climate and sustainability limits. *Geosci. Model Dev.* **2021**, *14*, 6571–6603. [CrossRef]
75. Riahi, K.; Van Vuuren, D.P.; Kriegler, E.; Edmonds, J.; O'Neill, B.C.; Fujimori, S.; Bauer, N.; Calvin, K.; Dellink, R.; Fricko, O.; et al. The Shared Socioeconomic Pathways and their energy, land use, and greenhouse gas emissions implications: An overview. *Glob. Environ. Change* **2017**, *42*, 153–168. [CrossRef]

Disclaimer/Publisher's Note: The statements, opinions and data contained in all publications are solely those of the individual author(s) and contributor(s) and not of MDPI and/or the editor(s). MDPI and/or the editor(s) disclaim responsibility for any injury to people or property resulting from any ideas, methods, instructions or products referred to in the content.